UNIVERSIDAD DE CONCEPCIÓN

Centro de Investigación en Ingeniería Matemática (CI^{2}MA)

A Banach spaces-based mixed finite element method for the stationary convective Brinkman-Forchheimer problem

Sergio Caucao, Gabriel N. Gatica,
Luis F. Gatica

PREPRINT 2023-10

SERIE DE PRE-PUBLICACIONES

A Banach spaces-based mixed finite element method for the stationary convective Brinkman–Forchheimer problem*

Sergio Caucao† Gabriel N. Gatica‡ Luis F. Gatica§

Abstract

We propose and analyze a new mixed finite element method for the nonlinear problem given by the stationary convective Brinkman–Forchheimer equations. In addition to the original fluid variables, the pseudostress is introduced as an auxiliary unknown, and then the incompressibility condition is used to eliminate the pressure, which is computed afterwards by a postprocessing formula depending on the aforementioned tensor and the velocity. As a consequence, we obtain a mixed variational formulation consisting of a nonlinear perturbation of, in turn, a perturbed saddle point problem in a Banach spaces framework. In this way, and differently from the techniques previously developed for this model, no augmentation procedure needs to be incorporated into the formulation nor into the solvability analysis. The resulting non-augmented scheme is then written equivalently as a fixed-point equation, so that recently established solvability results for perturbed saddle-point problems in Banach spaces, along with the well-known Banach–Nečas–Babuška and Banach theorems, are applied to prove the well-posedness of the continuous and discrete systems. The finite element discretization involves Raviart–Thomas elements of order $k \geq 0$ for the pseudostress tensor and discontinuous piecewise polynomial elements of degree $\leq k$ for the velocity. Stability, convergence, and optimal *a priori* error estimates for the associated Galerkin scheme are obtained. Numerical examples confirm the theoretical rates of convergence and illustrate the performance and flexibility of the method. In particular, the case of flow through a 2D porous media with fracture networks is considered.

Key words: convective Brinkman–Forchheimer equations, pseudoestress-velocity formulation, fixed point theory, perturbed saddle-point, mixed finite elements, *a priori* error analysis

Mathematics subject classifications (2000): 65N30, 65N12, 65N15, 35Q79, 80A20, 76R05, 76D07

1 Introduction

The phenomenon of flow of fluids through highly porous media at higher Reynolds numbers has a wide range of applications, including processes arising in environmental, chemical, and petroleum engineer-

*This research was supported by ANID-Chile through the projects Centro de Modelamiento Matemático (FB210005), Anillo of Computational Mathematics for Desalination Processes (ACT210087), Fondecyt 11220393, and Fondecyt 1181748; by Grupo de Investigación en Análisis Numérico y Cálculo Científico (GIANuC^2), Universidad Católica de la Santísima Concepción; and by Centro de Investigación en Ingeniería Matemática (CI^{2}MA), Universidad de Concepción.

†GIANuC^2 and Departamento de Matemática y Física Aplicadas, Universidad Católica de la Santísima Concepción, Casilla 297, Concepción, Chile, email: scaucao@ucsc.cl.

‡CI^{2}MA and Departamento de Ingeniería Matemática, Universidad de Concepción, Casilla 160-C, Concepción, Chile, email: ggatica@ci2ma.udec.cl.

§GIANuC^2 and Departamento de Matemática y Física Aplicadas, Universidad Católica de la Santísima Concepción, Casilla 297, Concepción, Chile, and CI^{2}MA, Universidad de Concepción, Casilla 160-C, Concepción, Chile, email: lgatica@ucsc.cl.

ing. In particular, fast flows in the subsurface may occur in fractured or vuggy aquifers or reservoirs, as well as near injection and production wells during groundwater remediation or hydrocarbon production. Most of the investigations in porous media have mainly focused on the use of Darcy's law, which represents a simple linear relationship between the flow rate and the pressure drop in a porous medium. However, this fundamental equation may be inaccurate for modeling fluid flow through porous media with high Reynolds numbers or through media with high porosity. To overcome this limitation, it is possible to consider the convective Brinkman–Forchheimer equations (see for instance [13] and [23]), where terms are added to Darcy's equation in order to take into account the above described physical aspects.

Concerning literature, we start mentioning some papers devoted to the mathematical analysis of the convective Brinkman–Forchheimer (CBF) equations in velocity-pressure formulation. To the authors' knowledge, [13] constitutes one of the first works in analyzing the continuous dependence of solutions of the CBF equations on the Forchheimer coefficient in H^1 norm. Later on, an approximation of solutions for the incompressible CBF equations via the artificial compressibility method was proposed and developed in [25], where a family of perturbed compressible CBF equations that approximate the incompressible CBF equations is introduced. Existence and convergence of solutions for the compressible CBF equations to the solutions of the incompressible CBF equations are also proved in [25]. In turn, the existence and uniqueness of an axisymmetric solution to the three-dimensional incompressible CBF equations were proved in [24]. Regarding numerical methods for the CBF equations we refer to [23] and [8]. In particular, the two-dimensional stationary CBF equations were analyzed in [23]. The focus of this work is on the well-posedness of the corresponding velocity-pressure variational formulation. In addition, error estimates for a mixed finite element approximation were obtained and a one-step Newton iteration algorithm initialized using a fixed-point iteration was proposed. Meanwhile, an augmented mixed pseudostress-velocity formulation was analyzed in [8]. In there, the well-posedness of the problem is achieved by combining a fixed-point strategy, the Lax–Milgram theorem, and the well-known Schauder and Banach fixed-point theorems. The corresponding numerical scheme is based on Raviart–Thomas spaces of order $k \geq 0$ for approximating the pseudostress tensor, whereas continuous piecewise polynomials of degree $k+1$ are employed for the velocity. Optimal *a priori* error estimates were obtained and also a suitable *a posteriori* error analysis were developed by the authors.

We point out that the augmented formulation introduced in [8], and the consequent use of classical Raviart–Thomas spaces and continuous piecewise polynomials to define the discrete scheme, are originated by the wish of performing the respective solvability analysis of the convective Brinkman–Forchheimer equations within a Hilbertian framework. However, it is well known that the introduction of additional terms into the formulation, while having some advantages, also leads to much more expensive schemes in terms of complexity and computational implementation. In order to overcome this, in recent years there has arisen an increasing development on Banach spaces-based mixed finite element methods to solve a wide family of single and coupled nonlinear problems in continuum mechanics. In particular, we refer to [6], [4], [12], [11], [10], [14], [1], [2], and [19], for the analysis of mixed formulations within a Banach framework of the Poisson, Navier–Stokes, Brinkman–Forchheimer, Boussinesq, coupled flow-transport, and Navier–Stokes–Brinkman equations. This kind of procedures shows two advantages at least: no augmentation is required, and the spaces to which the unknowns belong are the natural ones arising from the application of the Cauchy–Schwarz and Hölder inequalities to the terms resulting from the testing and integration by parts of the equations of the model. As a consequence, simpler and closer to the original physical model formulations are obtained.

The goal of the present paper is to continue extending the applicability of the aforementioned Banach spaces framework by proposing now a new mixed formulation, without any augmentation procedure, for the nonlinear problem studied in [8] (see also [13], [25], [23], and [24]). To this end, we proceed

as in [4] and introduce the pseudostress tensor as an auxiliary unknown, and subsequently eliminate the pressure unknown using the incompressibility condition. Then, similarly to [16], [7], and [19], we combine a fixed-point argument, the abstract results provided in [15], the Banach–Nečas–Babuška theorem, sufficiently small data assumptions, and the Banach theorem, to establish existence and uniqueness of solution of both the continuous and discrete formulations. In this regard, and since the formulation is similar to the ones analyzed in [15], [16], and [19], our present analysis certainly makes use of the corresponding results available there. In addition, applying an ad-hoc Strang-type lemma in Banach spaces established in [9], we are able to derive the corresponding *a priori* error estimates. Next, employing Raviart–Thomas spaces of order $k \geq 0$ for approximating the pseudostress tensor and discontinuous piecewise polynomials of degree $\leq k$ for the velocity, we prove that the method is convergent with optimal rates.

This work is organized as follows. The remainder of this section describes standard notation and functional spaces to be employed throughout the paper. In Section 2 we introduce the model problem and derive the mixed variational formulation in Banach spaces. Next, in Section 3 we establish the well-posedness of this continuous scheme. The corresponding Galerkin system is introduced and analyzed in Section 4, where the discrete analogue of the theory used in the continuous case is employed to prove existence and uniqueness of solution. In Section 5 we derive the corresponding *a priori* error estimate and establish the consequent rates of convergence. Finally, the performance of the method is illustrated in Section 6 with some numerical examples in 2D and 3D with and without manufactured solutions, which confirm the accuracy and flexibility of our non-augmented mixed finite element method.

Preliminary notations

Let $\Omega \subset \mathrm{R}^n, n \in \{2,3\}$, be a bounded domain with polyhedral boundary Γ, and let $\mathbf{n}$ be the outward unit normal vector on Γ. Standard notation will be adopted for Lebesgue spaces $\mathrm{L}^p(\Omega)$ and Sobolev spaces $\mathrm{W}^{s,p}(\Omega)$, with $s \in \mathrm{R}$ and $p > 1$, whose corresponding norms, either for the scalar, vectorial, or tensorial case, are written as $\|\cdot\|_{0,p;\Omega}$ and $\|\cdot\|_{s,p;\Omega}$, respectively. In addition, given a non-negative integer m, $\mathrm{W}^{m,2}(\Omega)$ is also denoted by $\mathrm{H}^m(\Omega)$, and the notations of its norm and seminorm are simplified to $\|\cdot\|_{m,\Omega}$ and $|\cdot|_{m,\Omega}$, respectively. By $\mathbf{M}$ and $\mathbb{M}$ we mean the corresponding vectorial and tensorial counterparts of the generic scalar functional space M, whereas M' represents its dual. In particular, we set $\mathbf{R} := \mathrm{R}^n$ and $\mathbb{R} := \mathrm{R}^{n\times n}$. In turn, for any vector fields $\mathbf{v} = (v_i)_{i=1,n}$ and $\mathbf{w} = (w_i)_{i=1,n}$, we define the gradient, divergence, and tensor product operators, as $\nabla\mathbf{v} := \left(\dfrac{\partial v_i}{\partial x_j}\right)_{i,j=1,n}$, $\mathrm{div}(\mathbf{v}) := \displaystyle\sum_{j=1}^{n} \frac{\partial v_j}{\partial x_j}$, and $\mathbf{v}\otimes\mathbf{w} := (v_i w_j)_{i,j=1,n}$. Also, for any tensor fields $\boldsymbol{\tau} = (\tau_{ij})_{i,j=1,n}$ and $\boldsymbol{\zeta} = (\zeta_{ij})_{i,j=1,n}$, we let $\mathbf{div}(\boldsymbol{\tau})$ be the usual divergence operator div acting along the rows of $\boldsymbol{\tau}$, and define the transpose, the trace, the tensor inner product, and the deviatoric tensor, respectively, as $\boldsymbol{\tau}^{\mathrm{t}} := (\tau_{ji})_{i,j=1,n}$, $\mathrm{tr}(\boldsymbol{\tau}) := \displaystyle\sum_{i=1}^{n} \tau_{ii}$, $\boldsymbol{\tau} : \boldsymbol{\zeta} := \displaystyle\sum_{i,j=1}^{n} \tau_{ij}\,\zeta_{ij}$, and $\boldsymbol{\tau}^{\mathrm{d}} := \boldsymbol{\tau} - \dfrac{1}{n}\,\mathrm{tr}(\boldsymbol{\tau})\,\mathbb{I}$, where $\mathbb{I}$ is the identity matrix in $\mathbb{R}$. In what follows, when no confusion arises, $|\cdot|$ denotes the Euclidean norm in $\mathbf{R}$ or $\mathbb{R}$. Furthermore, $\mathbf{H}^{1/2}(\Gamma)$ is the space of traces of functions of $\mathbf{H}^1(\Omega)$ and $\mathbf{H}^{-1/2}(\Gamma)$ is its dual, whereas $\langle\cdot,\cdot\rangle_\Gamma$ stands for the corresponding product of duality between $\mathbf{H}^{-1/2}(\Gamma)$ and $\mathbf{H}^{1/2}(\Gamma)$.

2 The continuous formulation

In this section we introduce the model problem and derive the corresponding weak formulation.

2.1 The model problem

In what follows we consider the model analyzed in [23] (see also [13, 25, 24, 8]), which is given by the steady convective Brinkman–Forchheimer equations. More precisely, given a body force $\mathbf{f}$, we focus on finding a velocity field $\mathbf{u}$, and a pressure field p, such that

$$\begin{array}{rcll} -\nu\,\Delta\mathbf{u} + (\nabla\mathbf{u})\mathbf{u} + \mathtt{D}\,\mathbf{u} + \mathtt{F}\,|\mathbf{u}|^{\rho-2}\mathbf{u} + \nabla p &=& \mathbf{f} & \text{in } \Omega\,, \\ \mathrm{div}(\mathbf{u}) &=& 0 & \text{in } \Omega\,, \\ \mathbf{u} &=& \mathbf{u}_{\mathrm{D}} & \text{on } \Gamma\,, \end{array} \tag{2.1}$$

where $\nu > 0$ is the Brinkman coefficient (or the effective viscosity), $\mathtt{D} > 0$ is the Darcy coefficient, $\mathtt{F} > 0$ is the Forchheimer coefficient, and ρ is a given number in $[3, 4]$. Owing to the incompressibility of the fluid, the datum $\mathbf{u}_{\mathrm{D}} \in \mathbf{H}^{1/2}(\Gamma)$ must satisfy the compatibility condition

$$\int_\Gamma \mathbf{u}_{\mathrm{D}} \cdot \mathbf{n} \,=\, 0\,. \tag{2.2}$$

In addition, due to the pressure-dependent term in the first equation of (2.1), and in order to guarantee uniqueness of p, this unknown will be sought in the space

$$\mathrm{L}^2_0(\Omega) \,:=\, \left\{ q \in \mathrm{L}^2(\Omega) : \quad \int_\Omega q = 0 \right\}\,.$$

Next, in order to derive a mixed formulation for (2.1), in which the Dirichlet boundary condition for the velocity becomes a natural one, we now proceed as in [5] (see similar approaches in [20, 10, 4, 8]), and introduce as a further unknown the nonlinear pseudostress tensor $\boldsymbol{\sigma}$, which is defined by

$$\boldsymbol{\sigma} := \nu\,\nabla\mathbf{u} - (\mathbf{u}\otimes\mathbf{u}) - p\,\mathbb{I}\,. \tag{2.3}$$

In this way, applying the trace operator to $\boldsymbol{\sigma}$ and utilizing the incompressibility condition $\mathrm{div}(\mathbf{u}) = 0$ in Ω, one arrives at

$$p = -\frac{1}{n}\,\mathrm{tr}(\boldsymbol{\sigma} + \mathbf{u}\otimes\mathbf{u})\,. \tag{2.4}$$

Hence, replacing back (2.4) into (2.3), we find that (2.1) can be rewritten, equivalently, as follows: Find $(\boldsymbol{\sigma}, \mathbf{u})$ in suitable spaces to be indicated below such that

$$\begin{array}{rcll} \dfrac{1}{\nu}\,\boldsymbol{\sigma}^{\mathrm{d}} + \dfrac{1}{\nu}\,(\mathbf{u}\otimes\mathbf{u})^{\mathrm{d}} &=& \nabla\mathbf{u} & \text{in } \Omega\,, \\ \mathtt{D}\,\mathbf{u} + \mathtt{F}\,|\mathbf{u}|^{\rho-2}\mathbf{u} - \mathbf{div}(\boldsymbol{\sigma}) &=& \mathbf{f} & \text{in } \Omega\,, \\ \mathbf{u} &=& \mathbf{u}_{\mathrm{D}} & \text{on } \Gamma\,, \\ \displaystyle\int_\Omega \mathrm{tr}(\boldsymbol{\sigma} + \mathbf{u}\otimes\mathbf{u}) &=& 0\,. \end{array} \tag{2.5}$$

At this point we stress that, as suggested by (2.4), p is eliminated from the present formulation and computed afterwards in terms of $\boldsymbol{\sigma}$ and $\mathbf{u}$ by using that identity. This fact justifies the last equation in (2.5), which aims to ensure that the resulting p does belong to $\mathrm{L}^2_0(\Omega)$. Notice also that further variables of interest, such as the velocity gradient $\mathbf{G} := \nabla\mathbf{u}$, the vorticity $\boldsymbol{\omega} := \frac{1}{2}\left(\nabla\mathbf{u} - (\nabla\mathbf{u})^{\mathrm{t}}\right)$, and the shear stress tensor $\widetilde{\boldsymbol{\sigma}} = \nu\left(\nabla\mathbf{u} + (\nabla\mathbf{u})^{\mathrm{t}}\right) - p\,\mathbb{I}$, can be easily computed in terms of $\boldsymbol{\sigma}$ and $\mathbf{u}$ as well, namely

$$\mathbf{G} = \frac{1}{\nu}\left(\boldsymbol{\sigma}^{\mathrm{d}} + (\mathbf{u}\otimes\mathbf{u})^{\mathrm{d}}\right)\,, \quad \boldsymbol{\omega} = \frac{1}{2\,\nu}\left(\boldsymbol{\sigma} - \boldsymbol{\sigma}^{\mathrm{t}}\right)\,, \quad \text{and} \quad \widetilde{\boldsymbol{\sigma}} = \boldsymbol{\sigma}^{\mathrm{d}} + (\mathbf{u}\otimes\mathbf{u})^{\mathrm{d}} + \boldsymbol{\sigma}^{\mathrm{t}} + (\mathbf{u}\otimes\mathbf{u})\,. \tag{2.6}$$

2.2 The variational formulation

In this section we follow [4] and [16] (see also [6], [19]) to derive a Banach spaces-based mixed formulation for the problem given by (2.5), which, unlike [8], does not resort to any augmentation procedure. To this end, we test the first and second equations of (2.5) against functions $\boldsymbol{\tau}$ and $\mathbf{v}$ associated with the unknowns $\boldsymbol{\sigma}$ and $\mathbf{u}$, respectively, whence, using the identity $\boldsymbol{\sigma}^{\mathrm{d}} : \boldsymbol{\tau} = \boldsymbol{\sigma}^{\mathrm{d}} : \boldsymbol{\tau}^{\mathrm{d}}$, we formally get

$$\frac{1}{\nu}\int_\Omega \boldsymbol{\sigma}^{\mathrm{d}} : \boldsymbol{\tau}^{\mathrm{d}} \,-\, \int_\Omega \nabla\mathbf{u} : \boldsymbol{\tau} \,+\, \frac{1}{\nu}\int_\Omega (\mathbf{u}\otimes\mathbf{u})^{\mathrm{d}} : \boldsymbol{\tau} \,=\, 0\,, \tag{2.7}$$

$$\int_\Omega \mathbf{v}\cdot\mathbf{div}(\boldsymbol{\sigma}) \,-\, \mathtt{D}\int_\Omega \mathbf{u}\cdot\mathbf{v} \,-\, \mathtt{F}\int_\Omega |\mathbf{u}|^{\rho-2}\mathbf{u}\cdot\mathbf{v} \,=\, -\int_\Omega \mathbf{f}\cdot\mathbf{v}\,. \tag{2.8}$$

Notice here that the first term of (2.7) is well-defined for $\boldsymbol{\sigma},\ \boldsymbol{\tau} \in \mathbb{L}^2(\Omega)$. In turn, applying the Hölder and Cauchy–Schwarz inequalities, and the Sobolev embedding of $\mathbf{L}^4(\Omega)$ into $\mathbf{L}^{2\,(\rho-2)}(\Omega)$, with $\rho \in [3,4]$, we find that the convective and Forchheimer terms, given by the third expressions in (2.7) and (2.8), can be bounded, respectively, as

$$\left|\int_\Omega (\mathbf{w}\otimes\mathbf{u})^{\mathrm{d}} : \boldsymbol{\tau}\right| \,\leq\, \|\mathbf{w}\|_{0,4;\Omega}\,\|\mathbf{u}\|_{0,4;\Omega}\,\|\boldsymbol{\tau}\|_{0,\Omega} \tag{2.9}$$

and

$$\left|\int_\Omega |\mathbf{w}|^{\rho-2}\mathbf{u}\cdot\mathbf{v}\right| \,\leq\, \|\mathbf{w}\|^{\rho-2}_{0,2(\rho-2);\Omega}\,\|\mathbf{u}\|_{0,4;\Omega}\,\|\mathbf{v}\|_{0,4;\Omega} \,\leq\, |\Omega|^{(4-\rho)/4}\,\|\mathbf{w}\|^{\rho-2}_{0,4;\Omega}\,\|\mathbf{u}\|_{0,4;\Omega}\,\|\mathbf{v}\|_{0,4;\Omega}\,, \tag{2.10}$$

which shows that they are well-defined for all $\mathbf{w},\ \mathbf{u},\ \mathbf{v} \in \mathbf{L}^4(\Omega)$ and for all $\boldsymbol{\tau} \in \mathbb{L}^2(\Omega)$. In addition, the fact that $\mathbf{L}^4(\Omega)$ is certainly contained in $\mathbf{L}^2(\Omega)$ guarantees that the second term in (2.8) makes sense as well. Next, knowing the space in which $\mathbf{v}$ is taken, we deduce that the source term of (2.8) makes sense if $\mathbf{f}$ belongs to $\mathbf{L}^{4/3}(\Omega)$, which is assumed from now on, whereas the first term of (2.8) is well-defined if $\mathbf{div}(\boldsymbol{\sigma})$ lies in $\mathbf{L}^{4/3}(\Omega)$ as well, and thus initially we look for $\boldsymbol{\sigma}$ in the Banach space

$$\mathbb{H}(\mathbf{div}_{4/3};\Omega) := \left\{\boldsymbol{\zeta} \in \mathbb{L}^2(\Omega) : \quad \mathbf{div}(\boldsymbol{\zeta}) \in \mathbf{L}^{4/3}(\Omega)\right\},$$

which is equipped with the norm $\|\boldsymbol{\zeta}\|_{\mathbf{div}_{4/3};\Omega} := \|\boldsymbol{\zeta}\|_{0,\Omega} + \|\mathbf{div}(\boldsymbol{\zeta})\|_{0,4/3;\Omega}$. Moreover, choosing $\mathbb{H}(\mathbf{div}_{4/3};\Omega)$ as the space to which the test functions $\boldsymbol{\tau}$ also belong, and assuming originally that $\mathbf{u} \in \mathbf{H}^1(\Omega)$, we can integrate by parts the second term in (2.7), so that, using the Dirichlet boundary condition $\mathbf{u} = \mathbf{u}_{\mathrm{D}}$ on Γ, that equation becomes

$$\frac{1}{\nu}\int_\Omega \boldsymbol{\sigma}^{\mathrm{d}} : \boldsymbol{\tau}^{\mathrm{d}} \,+\, \int_\Omega \mathbf{u}\cdot\mathbf{div}(\boldsymbol{\tau}) \,+\, \frac{1}{\nu}\int_\Omega (\mathbf{u}\otimes\mathbf{u})^{\mathrm{d}} : \boldsymbol{\tau} \,=\, \langle\boldsymbol{\tau}\mathbf{n}, \mathbf{u}_{\mathrm{D}}\rangle_\Gamma \quad \forall\,\boldsymbol{\tau} \in \mathbb{H}(\mathbf{div}_{4/3};\Omega)\,. \tag{2.11}$$

According to the previous analysis, the weak formulation of the convective Brinkman–Forchheimer problem (2.5) reduces at first instance to: Find $(\boldsymbol{\sigma},\mathbf{u}) \in \mathbb{H}(\mathbf{div}_{4/3};\Omega)\times\mathbf{L}^4(\Omega)$ such that $\int_\Omega \mathrm{tr}(\boldsymbol{\sigma}+\mathbf{u}\otimes\mathbf{u}) = 0$, and both (2.11) and (2.8) hold for all $(\boldsymbol{\tau},\mathbf{v}) \in \mathbb{H}(\mathbf{div}_{4/3};\Omega)\times\mathbf{L}^4(\Omega)$. However, similarly as in [4] (see also [14, 10, 11]), it is convenient to consider the decomposition

$$\mathbb{H}(\mathbf{div}_{4/3};\Omega) \,=\, \mathbb{H}_0(\mathbf{div}_{4/3};\Omega)\oplus\mathrm{R}\,\mathbb{I}\,, \tag{2.12}$$

where

$$\mathbb{H}_0(\mathbf{div}_{4/3};\Omega) \,:=\, \left\{\boldsymbol{\tau} \in \mathbb{H}(\mathbf{div}_{4/3};\Omega) : \quad \int_\Omega \mathrm{tr}(\boldsymbol{\tau}) = 0\right\},$$

thanks to which each $\boldsymbol{\tau} \in \mathbb{H}(\mathbf{div}_{4/3};\Omega)$ can be uniquely decomposed as

$$\boldsymbol{\tau} = \boldsymbol{\tau}_0 + d_0\,\mathbb{I} \quad \text{with} \quad \boldsymbol{\tau}_0 \in \mathbb{H}_0(\mathbf{div}_{4/3};\Omega) \quad \text{and} \quad d_0 := \frac{1}{n\,|\Omega|}\int_\Omega \mathrm{tr}(\boldsymbol{\tau}) \in \mathrm{R}\,.$$

In particular, using that $\displaystyle\int_\Omega \mathrm{tr}(\boldsymbol{\sigma}) = -\int_\Omega \mathrm{tr}(\mathbf{u}\otimes\mathbf{u})$, we obtain

$$\boldsymbol{\sigma} = \boldsymbol{\sigma}_0 + c_0\,\mathbb{I} \quad \text{with} \quad \boldsymbol{\sigma}_0 \in \mathbb{H}_0(\mathbf{div}_{4/3};\Omega) \quad \text{and} \quad c_0 := -\frac{1}{n\,|\Omega|}\int_\Omega \mathrm{tr}(\mathbf{u}\otimes\mathbf{u}) \in \mathrm{R}\,, \tag{2.13}$$

which says that c_0 is know explicitly in terms of $\mathbf{u}$. Therefore, in order to fully determine $\boldsymbol{\sigma}$, it only remains to find its $\mathbb{H}_0(\mathbf{div}_{4/3};\Omega)$-component $\boldsymbol{\sigma}_0$, which is renamed from now on simply as $\boldsymbol{\sigma}$.

Furthermore, using the compatibility condition (2.2), we observe that both sides of (2.11) explicitly vanish when $\boldsymbol{\tau} \in \mathrm{R}\mathbb{I}$, and therefore testing against $\boldsymbol{\tau} \in \mathbb{H}(\mathbf{div}_{4/3};\Omega)$ is equivalent to doing it against $\boldsymbol{\tau} \in \mathbb{H}_0(\mathbf{div}_{4/3};\Omega)$. Hence, bearing in mind the foregoing discussion, we arrive at the following Banach spaces-based mixed formulation for the convective Brinkman–Forchheimer equations: Find $(\boldsymbol{\sigma},\mathbf{u}) \in \mathbb{H}_0(\mathbf{div}_{4/3};\Omega)\times\mathbf{L}^4(\Omega)$ such that

$$\begin{aligned} a(\boldsymbol{\sigma},\boldsymbol{\tau}) + b(\boldsymbol{\tau},\mathbf{u}) + \frac{1}{\nu}\int_\Omega (\mathbf{u}\otimes\mathbf{u})^{\mathrm{d}} : \boldsymbol{\tau} &= \langle \boldsymbol{\tau}\mathbf{n}, \mathbf{u}_{\mathrm{D}}\rangle_\Gamma \quad \forall\,\boldsymbol{\tau} \in \mathbb{H}_0(\mathbf{div}_{4/3};\Omega)\,, \\ b(\boldsymbol{\sigma},\mathbf{v}) - c(\mathbf{u},\mathbf{v}) - \mathtt{F}\int_\Omega |\mathbf{u}|^{\rho-2}\mathbf{u}\cdot\mathbf{v} &= -\int_\Omega \mathbf{f}\cdot\mathbf{v} \quad \forall\,\mathbf{v} \in \mathbf{L}^4(\Omega)\,, \end{aligned} \tag{2.14}$$

where, the bilinear forms $a : \mathbb{H}_0(\mathbf{div}_{4/3};\Omega)\times\mathbb{H}_0(\mathbf{div}_{4/3};\Omega) \to \mathrm{R}$, $b : \mathbb{H}_0(\mathbf{div}_{4/3};\Omega)\times\mathbf{L}^4(\Omega) \to \mathrm{R}$, and $c : \mathbf{L}^4(\Omega)\times\mathbf{L}^4(\Omega) \to \mathrm{R}$, are defined as

$$a(\boldsymbol{\zeta},\boldsymbol{\tau}) := \frac{1}{\nu}\int_\Omega \boldsymbol{\zeta}^{\mathrm{d}} : \boldsymbol{\tau}^{\mathrm{d}}\,, \quad b(\boldsymbol{\tau},\mathbf{v}) := \int_\Omega \mathbf{v}\cdot\mathbf{div}(\boldsymbol{\tau})\,, \quad \text{and} \quad c(\mathbf{z},\mathbf{v}) := \mathtt{D}\int_\Omega \mathbf{z}\cdot\mathbf{v}\,, \tag{2.15}$$

for all $(\boldsymbol{\zeta},\mathbf{z}),(\boldsymbol{\tau},\mathbf{v}) \in \mathbb{H}_0(\mathbf{div}_{4/3};\Omega)\times\mathbf{L}^4(\Omega)$. Equivalently, defining the space $\mathbf{X} := \mathbb{H}_0(\mathbf{div}_{4/3};\Omega)\times\mathbf{L}^4(\Omega)$ equipped with the product norm

$$\|(\boldsymbol{\tau},\mathbf{v})\|_{\mathbf{X}} := \|\boldsymbol{\tau}\|_{\mathbf{div}_{4/3};\Omega} + \|\mathbf{v}\|_{0,4;\Omega} \quad \forall\,(\boldsymbol{\tau},\mathbf{v}) \in \mathbf{X}\,,$$

and introducing, for each $\mathbf{w} \in \mathbf{L}^4(\Omega)$, the bilinear form $\mathbf{A}_{\mathbf{w}} : \mathbf{X}\times\mathbf{X} \to \mathrm{R}$ defined by

$$\mathbf{A}_{\mathbf{w}}((\boldsymbol{\zeta},\mathbf{z}),(\boldsymbol{\tau},\mathbf{v})) := \mathbf{A}((\boldsymbol{\zeta},\mathbf{z}),(\boldsymbol{\tau},\mathbf{v})) + \mathbf{B}_{\mathbf{w}}((\boldsymbol{\zeta},\mathbf{z}),(\boldsymbol{\tau},\mathbf{v}))\,, \tag{2.16}$$

with

$$\mathbf{A}((\boldsymbol{\zeta},\mathbf{z}),(\boldsymbol{\tau},\mathbf{v})) := a(\boldsymbol{\zeta},\boldsymbol{\tau}) + b(\boldsymbol{\tau},\mathbf{z}) + b(\boldsymbol{\zeta},\mathbf{v}) - c(\mathbf{z},\mathbf{v})\,, \quad \text{and} \tag{2.17}$$

$$\mathbf{B}_{\mathbf{w}}((\boldsymbol{\zeta},\mathbf{z}),(\boldsymbol{\tau},\mathbf{v})) := \frac{1}{\nu}\int_\Omega (\mathbf{w}\otimes\mathbf{z})^{\mathrm{d}} : \boldsymbol{\tau} - \mathtt{F}\int_\Omega |\mathbf{w}|^{\rho-2}\mathbf{z}\cdot\mathbf{v}\,, \tag{2.18}$$

for all $(\boldsymbol{\zeta},\mathbf{z}),(\boldsymbol{\tau},\mathbf{v}) \in \mathbf{X}$, we deduce that (2.14) can be re-stated as: Find $(\boldsymbol{\sigma},\mathbf{u}) \in \mathbf{X}$ such that

$$\mathbf{A}_{\mathbf{u}}((\boldsymbol{\sigma},\mathbf{u}),(\boldsymbol{\tau},\mathbf{v})) = \mathbf{F}(\boldsymbol{\tau},\mathbf{v}) \quad \forall\,(\boldsymbol{\tau},\mathbf{v}) \in \mathbf{X}\,, \tag{2.19}$$

where $\mathbf{F} \in \mathbf{X}'$ is defined by

$$\mathbf{F}(\boldsymbol{\tau},\mathbf{v}) := \langle \boldsymbol{\tau}\mathbf{n}, \mathbf{u}_{\mathrm{D}}\rangle_\Gamma - \int_\Omega \mathbf{f}\cdot\mathbf{v} \quad \forall\,(\boldsymbol{\tau},\mathbf{v}) \in \mathbf{X}\,. \tag{2.20}$$

Our next goal is to analyze the solvability of (2.19) (equivalently, that of (2.14)), which can be seen as a nonlinear perturbation of, in turn, the perturbed saddle-point formulation in Banach spaces determined by the bilinear form $\mathbf{A}$ (equivalently, by the bilinear forms a, b, and c).

3 Analysis of the continuous problem

In this section we apply the abstract result provided by [15, Theorem 3.4], which establishes sufficient conditions for the well-posedness of a perturbed saddle-point problem in Banach spaces, along with the Banach–Nečas–Babuška theorem (cf. [17, Theorem 2.6]), which is the Banach version of the generalized Lax–Milgram lemma in Hilbert spaces (cf. [18, Theorem 1.1]), and the classical Banach fixed-point theorem, to prove the well-posedness of (2.19) under smallness assumptions on the data.

3.1 Preliminaries

Here we establish the stability properties of the forms involved in (2.19). We begin by observing, thanks to the Cauchy–Schwarz and Hölder inequalities, that the bilinear forms $a : \mathbb{H}_0(\mathbf{div}_{4/3};\Omega) \times \mathbb{H}_0(\mathbf{div}_{4/3};\Omega) \to \mathrm{R}$, $b : \mathbb{H}_0(\mathbf{div}_{4/3};\Omega) \times \mathbf{L}^4(\Omega) \to \mathrm{R}$, and $c : \mathbf{L}^4(\Omega) \times \mathbf{L}^4(\Omega) \to \mathrm{R}$ are bounded as indicated in what follows

$$\begin{aligned} |a(\boldsymbol{\zeta},\boldsymbol{\tau})| &\leq \frac{1}{\nu}\,\|\boldsymbol{\zeta}\|_{\mathbf{div}_{4/3};\Omega}\,\|\boldsymbol{\tau}\|_{\mathbf{div}_{4/3};\Omega} \qquad \forall\,\boldsymbol{\zeta},\boldsymbol{\tau} \in \mathbb{H}_0(\mathbf{div}_{4/3};\Omega)\,, \\ |b(\boldsymbol{\tau},\mathbf{v})| &\leq \|\boldsymbol{\tau}\|_{\mathbf{div}_{4/3};\Omega}\,\|\mathbf{v}\|_{0,4;\Omega} \qquad \forall\,(\boldsymbol{\tau},\mathbf{v}) \in \mathbf{X}\,, \\ |c(\mathbf{z},\mathbf{v})| &\leq \mathtt{D}\,|\Omega|^{1/2}\,\|\mathbf{z}\|_{0,4;\Omega}\,\|\mathbf{v}\|_{0,4;\Omega} \qquad \forall\,\mathbf{z},\mathbf{v} \in \mathbf{L}^4(\Omega)\,, \end{aligned} \tag{3.1}$$

which, together with the definition of the bilinear form $\mathbf{A}$ (cf. (2.17)) and simple computations, yields

$$\big|\mathbf{A}((\boldsymbol{\zeta},\mathbf{z}),(\boldsymbol{\tau},\mathbf{v}))\big| \leq C_{\mathbf{A}}\,\|(\boldsymbol{\zeta},\mathbf{z})\|_{\mathbf{X}}\,\|(\boldsymbol{\tau},\mathbf{v})\|_{\mathbf{X}} \quad \forall\,(\boldsymbol{\zeta},\mathbf{z}),(\boldsymbol{\tau},\mathbf{v}) \in \mathbf{X}\,, \tag{3.2}$$

with $C_{\mathbf{A}}$ depending on $\nu, \mathtt{D}$, and $|\Omega|$. In turn, using (2.9)–(2.10), and performing some algebraic manipulations, we deduce from (2.18) that for each $\mathbf{w} \in \mathbf{L}^4(\Omega)$ the bilinear form $\mathbf{B}_{\mathbf{w}}$ is bounded, namely

$$\begin{aligned} \big|\mathbf{B}_{\mathbf{w}}((\boldsymbol{\zeta},\mathbf{z}),(\boldsymbol{\tau},\mathbf{v}))\big| &\leq \left\{\frac{1}{\nu}\|\mathbf{w}\|_{0,4;\Omega} + \mathtt{F}\,|\Omega|^{(4-\rho)/4}\,\|\mathbf{w}\|_{0,4;\Omega}^{\rho-2}\right\}\,\|\mathbf{z}\|_{0,4;\Omega}\,\|(\boldsymbol{\tau},\mathbf{v})\|_{\mathbf{X}} \\ &\leq \left\{\frac{1}{\nu}\|\mathbf{w}\|_{0,4;\Omega} + \mathtt{F}\,|\Omega|^{(4-\rho)/4}\,\|\mathbf{w}\|_{0,4;\Omega}^{\rho-2}\right\}\,\|(\boldsymbol{\zeta},\mathbf{z})\|_{\mathbf{X}}\,\|(\boldsymbol{\tau},\mathbf{v})\|_{\mathbf{X}} \end{aligned} \tag{3.3}$$

for all $(\boldsymbol{\zeta},\mathbf{z}),(\boldsymbol{\tau},\mathbf{v}) \in \mathbf{X}$.

On the other hand, using the continuity of the normal trace operator in $\mathbb{H}(\mathbf{div}_{4/3};\Omega)$, and applying Hölder's inequality, it is readily seen that $\mathbf{F}$ (cf. (2.20)) is bounded as well, that is

$$\big|\mathbf{F}(\boldsymbol{\tau},\mathbf{v})\big| \leq C_{\mathbf{F}}\left\{\|\mathbf{f}\|_{0,4/3;\Omega} + \|\mathbf{u}_{\mathrm{D}}\|_{1/2,\Gamma}\right\}\,\|(\boldsymbol{\tau},\mathbf{v})\|_{\mathbf{X}} \quad \forall\,(\boldsymbol{\tau},\mathbf{v}) \in \mathbf{X}\,, \tag{3.4}$$

where $C_{\mathbf{F}} := \max\{1, \|\mathbf{i}_4\|\}$ and $\|\mathbf{i}_4\|$ is the norm of the continuous injection $\mathbf{i}_4$ of $\mathbf{H}^1(\Omega)$ into $\mathbf{L}^4(\Omega)$.

3.2 The perturbed saddle-point formulation

We now focus on showing that [15, Theorem 3.4] can be applied to the bilinear form $\mathbf{A}$ (cf. (2.17)), equivalently that the bilinear forms a, b, and c satisfy the assumptions of that abstract result. Indeed, it is clear from (3.1) that the bilinears forms a, b, and c are all bounded. In addition, we notice from the definitions of a and c (cf. (2.15)) that they are both symmetric and satisfy

$$a(\boldsymbol{\tau},\boldsymbol{\tau}) = \frac{1}{\nu}\,\|\boldsymbol{\tau}^{\mathrm{d}}\|_{0,\Omega}^2 \geq 0 \quad \forall\,\boldsymbol{\tau} \in \mathbb{H}_0(\mathbf{div}_{4/3};\Omega) \quad \text{and}$$

$$c(\mathbf{v},\mathbf{v}) = \mathtt{D}\,\|\mathbf{v}\|_{0,\Omega}^2 \geq 0 \quad \forall\,\mathbf{v} \in \mathbf{L}^4(\Omega)\,,$$

which yields the hypothesis **i)** of [15, Theorem 3.4]. On the other hand, we recall that a slight modification of the proof of [18, Lemma 2.3] (see also [3, Proposition IV.3.1]) allows to show the existence of a constant $c_1 > 0$, depending only on Ω, such that (cf. [4, Lemma 3.2])

$$c_1 \|\boldsymbol{\tau}\|_{0,\Omega} \leq \|\boldsymbol{\tau}^{\mathrm{d}}\|_{0,\Omega} + \|\mathbf{div}(\boldsymbol{\tau})\|_{0,4/3;\Omega} \quad \forall\, \boldsymbol{\tau} \in \mathbb{H}_0(\mathbf{div}_{4/3};\Omega)\,. \tag{3.5}$$

Next, noting that the null space $\mathbf{V}$ of the operator $\mathbf{B}$ induced by b is given by

$$\mathbf{V} = \Big\{ \boldsymbol{\tau} \in \mathbb{H}_0(\mathbf{div}_{4/3};\Omega) : \quad \mathbf{div}(\boldsymbol{\tau}) = \mathbf{0} \Big\}\,,$$

we readily see, bearing in mind the definition of a (cf. (2.15)) and applying (3.5), that

$$a(\boldsymbol{\tau},\boldsymbol{\tau}) = \frac{1}{\nu}\,\|\boldsymbol{\tau}^{\mathrm{d}}\|_{0,\Omega}^2 \geq \alpha\,\|\boldsymbol{\tau}\|_{\mathbf{div}_{4/3};\Omega}^2 \quad \forall\, \boldsymbol{\tau} \in \mathbf{V}\,, \tag{3.6}$$

with $\alpha := \frac{c_1^2}{\nu}$, from which it follows that a satisfies the continuous inf-sup condition on $\mathbf{V}$, thus verifying the hypothesis **ii)** of [15, Theorem 3.4]. Finally, denoting by $C_P > 0$ the Poincaré constant yielding the equivalence between $\|\cdot\|_{1,\Omega}$ and $|\cdot|_{1,\Omega}$ in $\mathbf{H}^1_0(\Omega)$, we know from [4, Lemma 3.3] that there holds the continuous inf-sup condition for b, that is

$$\sup_{\mathbf{0}\neq\boldsymbol{\tau}\in\mathbb{H}_0(\mathbf{div}_{4/3};\Omega)} \frac{b(\boldsymbol{\tau},\mathbf{v})}{\|\boldsymbol{\tau}\|_{\mathbf{div}_{4/3};\Omega}} \geq \beta\,\|\mathbf{v}\|_{0,4;\Omega} \quad \forall\, \mathbf{v} \in \mathbf{L}^4(\Omega)\,,$$

with $\beta := \big(n + n\|\mathbf{i}_4\|^2\, C_P^2\big)^{-1/2}$, which constitutes the verification of the respective hypothesis **iii)** of [15, Theorem 3.4].

Having proved that a, b, and c verify the assumptions of [15, Theorem 3.4], we deduce that the bilinear form $\mathbf{A}$ (cf. (2.17)) satisfies a corresponding global inf-sup condition, which means that there exists a constant $\gamma > 0$, depending only on ν, $\mathtt{D}$, $|\Omega|$, α, and β, such that

$$\sup_{\mathbf{0}\neq(\boldsymbol{\tau},\mathbf{v})\in\mathbf{X}} \frac{\mathbf{A}((\boldsymbol{\zeta},\mathbf{z}),(\boldsymbol{\tau},\mathbf{v}))}{\|(\boldsymbol{\tau},\mathbf{v})\|_{\mathbf{X}}} \geq \gamma\,\|(\boldsymbol{\zeta},\mathbf{z})\|_{\mathbf{X}} \quad \forall\, (\boldsymbol{\zeta},\mathbf{z}) \in \mathbf{X}\,. \tag{3.7}$$

3.3 A fixed point strategy

We begin the solvability analysis of (2.19) by defining the operator $\mathbf{T} : \mathbf{L}^4(\Omega) \to \mathbf{L}^4(\Omega)$ as

$$\mathbf{T}(\mathbf{w}) := \bar{\mathbf{u}} \quad \forall\, \mathbf{w} \in \mathbf{L}^4(\Omega)\,, \tag{3.8}$$

where $\bar{\mathbf{u}}$ is the second component of the unique solution (to be derived below) of the linear problem: Find $(\bar{\boldsymbol{\sigma}},\bar{\mathbf{u}}) \in \mathbf{X}$ such that

$$\mathbf{A}_{\mathbf{w}}((\bar{\boldsymbol{\sigma}},\bar{\mathbf{u}}),(\boldsymbol{\tau},\mathbf{v})) = \mathbf{F}(\boldsymbol{\tau},\mathbf{v}) \quad \forall\, (\boldsymbol{\tau},\mathbf{v}) \in \mathbf{X}\,. \tag{3.9}$$

It follows that (2.19) can be rewritten as the fixed-point equation: Find $\mathbf{u} \in \mathbf{L}^4(\Omega)$ such that

$$\mathbf{T}(\mathbf{u}) = \mathbf{u}\,, \tag{3.10}$$

so that, letting $(\bar{\boldsymbol{\sigma}},\bar{\mathbf{u}})$ be the solution of (3.9) with $\mathbf{w} := \mathbf{u}$, it is clear that $(\boldsymbol{\sigma},\mathbf{u}) := (\bar{\boldsymbol{\sigma}},\bar{\mathbf{u}}) \in \mathbf{X}$ is solution of (2.19), equivalently of (2.14).

The following result provides sufficient conditions under which the operator $\mathbf{T}$ (cf. (3.8)) is well-defined, or equivalently, the problem (3.9) is well-posed.

Lemma 3.1 *Let $r \in (0, r_0]$, with $r_0 = \min\{r_1, r_2\}$, and*

$$r_1 := \frac{\nu\,\gamma}{4} \quad \text{and} \quad r_2 := \left(\frac{\gamma}{4\,\mathtt{F}\,|\Omega|^{(4-\rho)/4}}\right)^{1/(\rho-2)}, \tag{3.11}$$

and let $\mathbf{f} \in \mathbf{L}^{4/3}(\Omega)$ and $\mathbf{u}_{\mathrm{D}} \in \mathbf{H}^{1/2}(\Gamma)$. Then, the problem (3.9) has a unique solution $(\bar{\boldsymbol{\sigma}}, \bar{\mathbf{u}}) \in \mathbf{X}$ for each $\mathbf{w} \in \mathbf{L}^4(\Omega)$ such that $\|\mathbf{w}\|_{0,4;\Omega} \leq r$, and hence $\mathbf{T}(\mathbf{w}) = \bar{\mathbf{u}} \in \mathbf{L}^4(\Omega)$ is well defined. Moreover, there holds

$$\|\mathbf{T}(\mathbf{w})\|_{0,4;\Omega} = \|\bar{\mathbf{u}}\|_{0,4;\Omega} \leq \|(\bar{\boldsymbol{\sigma}}, \bar{\mathbf{u}})\|_{\mathbf{X}} \leq \frac{2\,C_{\mathbf{F}}}{\gamma}\left\{\|\mathbf{f}\|_{0,4/3;\Omega} + \|\mathbf{u}_{\mathrm{D}}\|_{1/2,\Gamma}\right\}, \tag{3.12}$$

with $C_{\mathbf{F}}$ and γ satisfying (3.4) and (3.7), respectively.

Proof. We observe first from (2.16), (3.2), and (3.3) that for each $\mathbf{w} \in \mathbf{L}^4(\Omega)$, $\mathbf{A}_{\mathbf{w}}$ is clearly a bounded bilinear form. In turn, combining the inf-sup condition for $\mathbf{A}$ (cf. (3.7)) with the continuity bound of $\mathbf{B}_{\mathbf{w}}$ (cf. (3.3)), we find that

$$\begin{aligned}\sup_{\mathbf{0}\neq(\boldsymbol{\tau},\mathbf{v})\in\mathbf{X}} \frac{\mathbf{A}_{\mathbf{w}}((\boldsymbol{\zeta},\mathbf{z}),(\boldsymbol{\tau},\mathbf{v}))}{\|(\boldsymbol{\tau},\mathbf{v})\|_{\mathbf{X}}} &= \sup_{\mathbf{0}\neq(\boldsymbol{\tau},\mathbf{v})\in\mathbf{X}} \frac{\mathbf{A}((\boldsymbol{\zeta},\mathbf{z}),(\boldsymbol{\tau},\mathbf{v})) + \mathbf{B}_{\mathbf{w}}((\boldsymbol{\zeta},\mathbf{z}),(\boldsymbol{\tau},\mathbf{v}))}{\|(\boldsymbol{\tau},\mathbf{v})\|_{\mathbf{X}}} \\ &\geq \left\{\gamma - \left(\frac{1}{\nu}\,\|\mathbf{w}\|_{0,4;\Omega} + \mathtt{F}\,|\Omega|^{(4-\rho)/4}\|\mathbf{w}\|^{\rho-2}_{0,4;\Omega}\right)\right\}\,\|(\boldsymbol{\zeta},\mathbf{z})\|_{\mathbf{X}}\,,\end{aligned}$$

for all $(\boldsymbol{\zeta}, \mathbf{z}) \in \mathbf{X}$. Consequently, requiring now $\|\mathbf{w}\|_{0,4;\Omega} \leq r_0$, with $r_0 := \min\{r_1, r_2\}$ and r_1, r_2 as in (3.11), we get

$$\frac{1}{\nu}\,\|\mathbf{w}\|_{0,4;\Omega} \leq \frac{\gamma}{4} \quad \text{and} \quad \mathtt{F}\,|\Omega|^{(4-\rho)/4}\|\mathbf{w}\|^{\rho-2}_{0,4;\Omega} \leq \frac{\gamma}{4}\,,$$

which implies

$$\sup_{\mathbf{0}\neq(\boldsymbol{\tau},\mathbf{v})\in\mathbf{X}} \frac{\mathbf{A}_{\mathbf{w}}((\boldsymbol{\zeta},\mathbf{z}),(\boldsymbol{\tau},\mathbf{v}))}{\|(\boldsymbol{\tau},\mathbf{v})\|_{\mathbf{X}}} \geq \frac{\gamma}{2}\,\|(\boldsymbol{\zeta},\mathbf{z})\|_{\mathbf{X}} \quad \forall\,(\boldsymbol{\zeta},\mathbf{z}) \in \mathbf{X}\,. \tag{3.13}$$

Similarly, bearing in mind the symmetry of $\mathbf{A}$, using (3.7), and (3.3), and considering again $\mathbf{w} \in \mathbf{L}^4(\Omega)$ such that $\|\mathbf{w}\|_{0,4;\Omega} \leq r_0$, we deduce that

$$\sup_{(\boldsymbol{\zeta},\mathbf{z})\in\mathbf{X}} \mathbf{A}_{\mathbf{w}}((\boldsymbol{\zeta},\mathbf{z}),(\boldsymbol{\tau},\mathbf{v})) \geq \sup_{\mathbf{0}\neq(\boldsymbol{\zeta},\mathbf{z})\in\mathbf{X}} \frac{\mathbf{A}_{\mathbf{w}}((\boldsymbol{\zeta},\mathbf{z}),(\boldsymbol{\tau},\mathbf{v}))}{\|(\boldsymbol{\zeta},\mathbf{z})\|_{\mathbf{X}}} \geq \frac{\gamma}{2}\,\|(\boldsymbol{\tau},\mathbf{v})\|_{\mathbf{X}}$$

for all $(\boldsymbol{\tau}, \mathbf{v}) \in \mathbf{X}$, $(\boldsymbol{\tau}, \mathbf{v}) \neq \mathbf{0}$. Summing up, we have proved that for any $\mathbf{w} \in \mathbf{L}^4(\Omega)$ as indicated above, the bilinear form $\mathbf{A}_{\mathbf{w}}$ and the functional $\mathbf{F}$ satisfy the hypotheses of the Banach-Nečas-Babuška theorem (cf. [17, Theorem 2.6]), which guarantees the well-posedness of (3.9). Finally, applying (3.13) to $(\boldsymbol{\zeta}, \mathbf{z}) = (\bar{\boldsymbol{\sigma}}, \bar{\mathbf{u}})$, and then using (3.9) and the continuity bound of $\mathbf{F}$ (cf. (3.4)), we readily arrive at (3.12), which concludes the proof. □

3.4 Well-posedness of the continuous problem

Having proved the well-posedness of the problem (3.9), which ensures that the operator $\mathbf{T}$ is well defined, we now aim to establish the existence of a unique fixed point of the operator $\mathbf{T}$ (cf. (3.10)). For this purpose, in what follows we verify the hypothesis of the Banach fixed-point theorem.

The following result, which is a straightforward consequence of Lemma 3.1, establishes that $\mathbf{T}$ maps a ball into itself.

Lemma 3.2 *Given $r \in (0, r_0]$, with $r_0 := \min\{r_1, r_2\}$ and r_1, r_2 as in (3.11), we let $\mathbf{W}_r$ be the ball defined as*

$$\mathbf{W}_r := \Big\{ \mathbf{w} \in \mathbf{L}^4(\Omega) : \quad \|\mathbf{w}\|_{0,4;\Omega} \leq r \Big\}. \tag{3.14}$$

In addition, assume that

$$\frac{2\,C_{\mathbf{F}}}{\gamma} \Big\{ \|\mathbf{f}\|_{0,4/3;\Omega} + \|\mathbf{u}_{\mathrm{D}}\|_{1/2,\Gamma} \Big\} \leq r\,, \tag{3.15}$$

with $C_{\mathbf{F}}$ and γ satisfying (3.4) and (3.7), respectively. Then there holds $\mathbf{T}(\mathbf{W}_r) \subseteq \mathbf{W}_r$.

We continue by providing the Lipschitz continuity property of the operator $\mathbf{T}$. To that end, we first recall from [21, Lemma 5.3] that for each $p \geq 2$ there exists a constant $C(p) > 0$ such that

$$\big| |\mathbf{z}|^{p-2}\mathbf{z} - |\mathbf{y}|^{p-2}\mathbf{y} \big| \leq C(p) \big(|\mathbf{z}| + |\mathbf{y}| \big)^{p-2} |\mathbf{z} - \mathbf{y}| \quad \forall\, \mathbf{z},\, \mathbf{y} \in \mathbf{R}\,. \tag{3.16}$$

Then, given arbitrary $\mathbf{w}_1$, $\mathbf{w}_2 \in \mathbf{L}^4(\Omega)$, we apply (3.16) to the setting $p = \rho - 1 \in [2, 3]$, $\mathbf{z} = (|\mathbf{w}_1|, \mathbf{0})$, and $\mathbf{y} = (|\mathbf{w}_2|, \mathbf{0})$, with $\mathbf{0} \in \mathrm{R}^{n-1}$, denote $c_\rho := C(\rho - 1)$, and conclude that there holds

$$\begin{aligned} \big| |\mathbf{w}_1|^{\rho-2} - |\mathbf{w}_2|^{\rho-2} \big| &= \big| |\mathbf{w}_1|^{\rho-3}(|\mathbf{w}_1|, \mathbf{0}) - |\mathbf{w}_2|^{\rho-3}(|\mathbf{w}_2|, \mathbf{0}) \big| \\ &\leq c_\rho \big(|\mathbf{w}_1| + |\mathbf{w}_2| \big)^{\rho-3} |\mathbf{w}_1 - \mathbf{w}_2|\,. \end{aligned} \tag{3.17}$$

We are now in position to establish the announced result on $\mathbf{T}$.

Lemma 3.3 *Let $\rho \in [3, 4]$ and $r \in (0, r_0]$, with $r_0 := \min\{r_1, r_2\}$ and r_1, r_2 as in (3.11), and let $\mathbf{W}_r$ given by (3.14). Then, there holds*

$$\|\mathbf{T}(\mathbf{w}_1) - \mathbf{T}(\mathbf{w}_2)\|_{0,4;\Omega} \leq \big(1 + 2^{\rho-3} c_\rho \big) \frac{C_{\mathbf{F}}}{\gamma\, r_0} \Big\{ \|\mathbf{f}\|_{0,4/3;\Omega} + \|\mathbf{u}_{\mathrm{D}}\|_{1/2,\Gamma} \Big\} \|\mathbf{w}_1 - \mathbf{w}_2\|_{0,4;\Omega} \tag{3.18}$$

for all $\mathbf{w}_1$, $\mathbf{w}_2 \in \mathbf{W}_r$.

Proof. Given $\mathbf{w}_1, \mathbf{w}_2 \in \mathbf{W}_r$, we let $\bar{\mathbf{u}}_1 := \mathbf{T}(\mathbf{w}_1)$ and $\bar{\mathbf{u}}_2 := \mathbf{T}(\mathbf{w}_2)$. According to the definitions of $\mathbf{T}$ (cf. (3.9)) and the forms $\mathbf{A}_{\mathbf{w}}$ and $\mathbf{B}_{\mathbf{w}}$ (cf. (2.16), (2.18)), it follows that

$$\begin{aligned} \mathbf{A}_{\mathbf{w}_2}((\bar{\boldsymbol{\sigma}}_1, \bar{\mathbf{u}}_1) - (\bar{\boldsymbol{\sigma}}_2, \bar{\mathbf{u}}_2), (\boldsymbol{\tau}, \mathbf{v})) &= -(\mathbf{B}_{\mathbf{w}_1} - \mathbf{B}_{\mathbf{w}_2})((\bar{\boldsymbol{\sigma}}_1, \bar{\mathbf{u}}_1), (\boldsymbol{\tau}, \mathbf{v})) \\ &= \frac{1}{\nu} \int_\Omega \big((\mathbf{w}_2 - \mathbf{w}_1) \otimes \bar{\mathbf{u}}_1 \big)^{\mathtt{d}} : \boldsymbol{\tau} + \mathtt{F} \int_\Omega \big(|\mathbf{w}_1|^{\rho-2} - |\mathbf{w}_2|^{\rho-2} \big) \bar{\mathbf{u}}_1 \cdot \mathbf{v} \end{aligned}$$

for all $(\boldsymbol{\tau}, \mathbf{v}) \in \mathbf{X}$. Now, using (2.9), we readily obtain

$$\left| \frac{1}{\nu} \int_\Omega \big((\mathbf{w}_2 - \mathbf{w}_1) \otimes \bar{\mathbf{u}}_1 \big)^{\mathtt{d}} : \boldsymbol{\tau} \right| \leq \frac{1}{\nu} \|\mathbf{w}_1 - \mathbf{w}_2\|_{0,4;\Omega} \|\bar{\mathbf{u}}_1\|_{0,4;\Omega} \|\boldsymbol{\tau}\|_{0,\Omega}\,. \tag{3.19}$$

In turn, employing (3.17), Cauchy-Schwarz's inequality (twice), and the fact that the norm of the injection of $\mathbf{L}^4(\Omega)$ into $\mathbf{L}^t(\Omega)$, with $t \in (1, 4]$, is bounded by $|\Omega|^{(4-t)/(4t)}$, we deduce that

$$\begin{aligned} &\left| \mathtt{F} \int_\Omega \big(|\mathbf{w}_1|^{\rho-2} - |\mathbf{w}_2|^{\rho-2} \big) \bar{\mathbf{u}}_1 \cdot \mathbf{v} \right| \leq \mathtt{F}\, c_\rho \int_\Omega \big(|\mathbf{w}_1| + |\mathbf{w}_2| \big)^{\rho-3} |\mathbf{w}_1 - \mathbf{w}_2|\, |\bar{\mathbf{u}}_1|\, |\mathbf{v}| \\ &\leq \mathtt{F}\, c_\rho\, |\Omega|^{(4-\rho)/4} \big(\|\mathbf{w}_1\|_{0,4;\Omega} + \|\mathbf{w}_2\|_{0,4;\Omega} \big)^{\rho-3} \|\mathbf{w}_1 - \mathbf{w}_2\|_{0,4;\Omega} \|\bar{\mathbf{u}}_1\|_{0,4;\Omega} \|\mathbf{v}\|_{0,4;\Omega}\,. \end{aligned} \tag{3.20}$$

Hence, applying (3.13) with $\mathbf{w} = \mathbf{w}_2$ and $(\boldsymbol{\zeta}, \mathbf{z}) = (\bar{\boldsymbol{\sigma}}_1, \bar{\mathbf{u}}_1) - (\bar{\boldsymbol{\sigma}}_2, \bar{\mathbf{u}}_2)$, and then invoking (3.19) and (3.20), we readily get

$$\begin{aligned} \frac{\gamma}{2} \|(\bar{\boldsymbol{\sigma}}_1, \bar{\mathbf{u}}_1) - (\bar{\boldsymbol{\sigma}}_2, \bar{\mathbf{u}}_2)\|_{\mathbf{X}} &\leq \sup_{\mathbf{0} \neq (\boldsymbol{\tau}, \mathbf{v}) \in \mathbf{X}} \frac{-(\mathbf{B}_{\mathbf{w}_1} - \mathbf{B}_{\mathbf{w}_2})((\bar{\boldsymbol{\sigma}}_1, \bar{\mathbf{u}}_1), (\boldsymbol{\tau}, \mathbf{v}))}{\|(\boldsymbol{\tau}, \mathbf{v})\|_{\mathbf{X}}} \\ &\leq \left(\frac{1}{\nu} + \mathtt{F}\, c_\rho\, |\Omega|^{(4-\rho)/4} \left(\|\mathbf{w}_1\|_{0,4;\Omega} + \|\mathbf{w}_2\|_{0,4;\Omega} \right)^{\rho-3} \right) \|\bar{\mathbf{u}}_1\|_{0,4;\Omega}\, \|\mathbf{w}_1 - \mathbf{w}_2\|_{0,4;\Omega}\,. \end{aligned} \tag{3.21}$$

Then, noting from (3.11) that $\dfrac{1}{\nu} = \dfrac{\gamma}{4\, r_1}$ and $\mathtt{F}\, |\Omega|^{(4-\rho)/4} = \dfrac{\gamma}{4\, r_2^{\rho-2}}$, and using that both $\|\mathbf{w}_1\|_{0,4;\Omega}$ and $\|\mathbf{w}_2\|_{0,4;\Omega}$ are bounded, in particular, by r_2, (3.21) and simple algebraic computations lead to

$$\|(\bar{\boldsymbol{\sigma}}_1, \bar{\mathbf{u}}_1) - (\bar{\boldsymbol{\sigma}}_2, \bar{\mathbf{u}}_2)\|_{\mathbf{X}} \leq \frac{1}{2} \left(\frac{1}{r_1} + \frac{2^{\rho-3}\, c_\rho}{r_2} \right) \|\bar{\mathbf{u}}_1\|_{0,4;\Omega}\, \|\mathbf{w}_1 - \mathbf{w}_2\|_{0,4;\Omega}\,. \tag{3.22}$$

Finally, noting in (3.22) that both $1/r_1$ and $1/r_2$ are bounded by $1/r_0$ and bounding $\|\bar{\mathbf{u}}_1\|_{0,4;\Omega}$ by (3.12) instead of directly by r, we obtain (3.18) and conclude the proof. □

The main result concerning the solvability of (2.19) (equivalently of (2.14)) is established as follows.

Theorem 3.4 *Let $\rho \in [3,4]$ and $r \in (0, r_0]$, with $r_0 := \min\{r_1, r_2\}$ and r_1, r_2 as in* (3.11)*. Assume that the data satisfy* (3.15) *and*

$$\left(1 + 2^{\rho-3} c_\rho\right) \frac{C_{\mathbf{F}}}{\gamma\, r_0} \left\{ \|\mathbf{f}\|_{0,4/3;\Omega} + \|\mathbf{u}_{\mathrm{D}}\|_{1/2,\Gamma} \right\} < 1\,. \tag{3.23}$$

Then, there exists a unique $\mathbf{u} \in \mathbf{W}_r$ (cf. (3.14)*) fixed-point of operator $\mathbf{T}$. Equivalently,* (2.19) *has a unique solution $(\boldsymbol{\sigma}, \mathbf{u}) := (\bar{\boldsymbol{\sigma}}, \bar{\mathbf{u}}) \in \mathbf{X}$ with $\mathbf{u} \in \mathbf{W}_r$, where $(\bar{\boldsymbol{\sigma}}, \bar{\mathbf{u}})$ is the unique solution of* (3.9) *with $\mathbf{w} = \mathbf{u}$. Moreover, there holds*

$$\|(\boldsymbol{\sigma}, \mathbf{u})\|_{\mathbf{X}} \leq \frac{2\, C_{\mathbf{F}}}{\gamma} \left\{ \|\mathbf{f}\|_{0,4/3;\Omega} + \|\mathbf{u}_{\mathrm{D}}\|_{1/2,\Gamma} \right\}. \tag{3.24}$$

Proof. We begin by recalling from Lemma 3.2 that, under the assumption (3.15), $\mathbf{T}$ maps the ball $\mathbf{W}_r$ into itself, and hence, for each $\mathbf{w} \in \mathbf{W}_r$ we have that both $\|\mathbf{w}\|_{0,4;\Omega}$ and $\|\mathbf{T}(\mathbf{w})\|_{0,4;\Omega}$ are bounded by r. In turn, it is clear from Lemma 3.3 and hypothesis (3.23) that $\mathbf{T}$ is a contraction. Therefore, the Banach fixed-point theorem provides the existence of a unique fixed point $\mathbf{u} \in \mathbf{W}_r$ of $\mathbf{T}$, equivalently, the existence of a unique solution $(\boldsymbol{\sigma}, \mathbf{u}) \in \mathbf{X}$ of the problem (2.19) (equivalently of (2.14)), with $\mathbf{u} \in \mathbf{W}_r$. In addition, it is clear that the estimate (3.24) follows straightforwardly from (3.12), which finishes the proof. □

4 The Galerkin scheme

In this section we introduce and analyze the corresponding Galerkin method for the mixed formulation (2.19) (equivalently (2.14)).

4.1 Discrete setting

We begin by considering arbitrary finite dimensional subspaces $\widetilde{\mathbb{H}}_h^{\boldsymbol{\sigma}} \subseteq \mathbb{H}(\mathbf{div}_{4/3}; \Omega)$ and $\mathbf{H}_h^{\mathbf{u}} \subseteq \mathbf{L}^4(\Omega)$. Hereafter, $h := \max\left\{h_T : T \in \mathcal{T}_h\right\}$ stands for the size of a regular triangulation $\mathcal{T}_h$ of $\overline{\Omega}$ made up

of triangles T (when $n = 2$) or tetrahedra T (when $n = 3$) of diameter h_T. Specific finite element subspaces satisfying suitable hypotheses to be introduced in due course will be provided later on in Section 4.3. Then, letting

$$\mathbb{H}_h^{\boldsymbol{\sigma}} := \widetilde{\mathbb{H}}_h^{\boldsymbol{\sigma}} \cap \mathbb{H}_0(\mathbf{div}_{4/3};\Omega)\,, \tag{4.1}$$

the Galerkin scheme associated with (2.14) reads: Find $(\boldsymbol{\sigma}_h, \mathbf{u}_h) \in \mathbb{H}_h^{\boldsymbol{\sigma}} \times \mathbf{H}_h^{\mathbf{u}}$ such that

$$\begin{aligned} a(\boldsymbol{\sigma}_h, \boldsymbol{\tau}_h) + b(\boldsymbol{\tau}_h, \mathbf{u}_h) + \frac{1}{\nu}\int_\Omega (\mathbf{u}_h \otimes \mathbf{u}_h)^{\mathrm{d}} : \boldsymbol{\tau}_h &= \langle \boldsymbol{\tau}_h \mathbf{n}, \mathbf{u}_{\mathrm{D}} \rangle_\Gamma \quad \forall\, \boldsymbol{\tau}_h \in \mathbb{H}_h^{\boldsymbol{\sigma}}\,, \\ b(\boldsymbol{\sigma}_h, \mathbf{v}_h) - c(\mathbf{u}_h, \mathbf{v}_h) - \mathtt{F}\int_\Omega |\mathbf{u}_h|^{\mathrm{p}-2}\mathbf{u}_h \cdot \mathbf{v}_h &= -\int_\Omega \mathbf{f}\cdot\mathbf{v}_h \quad \forall\, \mathbf{v}_h \in \mathbf{H}_h^{\mathbf{u}}\,. \end{aligned} \tag{4.2}$$

Similarly, setting $\mathbf{X}_h := \mathbb{H}_h^{\boldsymbol{\sigma}} \times \mathbf{H}_h^{\mathbf{u}}$, the Galerkin scheme associated with (2.19), which is certainly equivalent to (4.2), becomes: Find $(\boldsymbol{\sigma}_h, \mathbf{u}_h) \in \mathbf{X}_h$ such that

$$\mathbf{A}_{\mathbf{u}_h}((\boldsymbol{\sigma}_h, \mathbf{u}_h), (\boldsymbol{\tau}_h, \mathbf{v}_h)) = \mathbf{F}(\boldsymbol{\tau}_h, \mathbf{v}_h) \quad \forall\, (\boldsymbol{\tau}_h, \mathbf{v}_h) \in \mathbf{X}_h\,. \tag{4.3}$$

The solvability of (4.3) (equivalently of (4.2)) is addressed below in Section 4.2 following analogous tools to those employed throughout Section 3, in particular using the discrete versions of [15, Theorem 3.4] and [17, Theorem 2.6], which are provided by [15, Theorem 3.5] and [17, Theorem 2.22], respectively.

4.2 Solvability Analysis

In this section we adopt the discrete version of the fixed-point strategy utilized in Section 3 to study the solvability of (4.3). To this end, we now let $\mathbf{T}_{\mathtt{d}} : \mathbf{H}_h^{\mathbf{u}} \to \mathbf{H}_h^{\mathbf{u}}$ be the operator defined by

$$\mathbf{T}_{\mathtt{d}}(\mathbf{w}_h) = \bar{\mathbf{u}}_h \quad \forall\, \mathbf{w}_h \in \mathbf{H}_h^{\mathbf{u}}\,,$$

where $(\bar{\boldsymbol{\sigma}}_h, \bar{\mathbf{u}}_h)$ is the unique solution of the problem arising from (4.3) after replacing $\mathbf{u}_h$ there by $\mathbf{w}_h$, that is: Find $(\bar{\boldsymbol{\sigma}}_h, \bar{\mathbf{u}}_h) \in \mathbf{X}_h$ such that

$$\mathbf{A}_{\mathbf{w}_h}((\bar{\boldsymbol{\sigma}}_h, \bar{\mathbf{u}}_h), (\boldsymbol{\tau}_h, \mathbf{v}_h)) = \mathbf{F}(\boldsymbol{\tau}_h, \mathbf{v}_h) \quad \forall\, (\boldsymbol{\tau}_h, \mathbf{v}_h) \in \mathbf{X}_h\,, \tag{4.4}$$

where the bilinear form $\mathbf{A}_{\mathbf{w}_h}$ and the functional $\mathbf{F}$ are defined in (2.16) (with $\mathbf{w}_h$ instead of $\mathbf{w}$) and (2.20), respectively. Therefore solving (4.3) is equivalent to seeking a fixed point of the operator $\mathbf{T}_{\mathtt{d}}$, that is: Find $\mathbf{u}_h \in \mathbf{H}_h^{\mathbf{u}}$ such that

$$\mathbf{T}_{\mathtt{d}}(\mathbf{u}_h) = \mathbf{u}_h\,, \tag{4.5}$$

so that, letting $(\bar{\boldsymbol{\sigma}}_h, \bar{\mathbf{u}}_h)$ be the solution of (4.4) with $\mathbf{w}_h := \mathbf{u}_h$, it is clear that $(\boldsymbol{\sigma}_h, \mathbf{u}_h) := (\bar{\boldsymbol{\sigma}}_h, \bar{\mathbf{u}}_h) \in \mathbf{X}_h$ is solution of (4.3), equivalently of (4.2).

In what follows we derive the preliminary results needed to address later on the solvabilities of (4.4) and (4.5), and hence of (4.3). Indeed, following a similar procedure to the one from Section 3, we first observe that the kernel $\mathbf{V}_h$ of $b|_{\mathbb{H}_h^{\boldsymbol{\sigma}} \times \mathbf{H}_h^{\mathbf{u}}}$ reduces to

$$\mathbf{V}_h := \Big\{ \boldsymbol{\tau}_h \in \mathbb{H}_h^{\boldsymbol{\sigma}} : \quad \int_\Omega \mathbf{v}_h \cdot \mathbf{div}(\boldsymbol{\tau}_h) = 0 \quad \forall\, \mathbf{v}_h \in \mathbb{H}_h^{\mathbf{u}} \Big\}\,.$$

Then, we introduce our first hypotheses on the finite element subspaces, namely

(**H.0**) $\widetilde{\mathbb{H}}_h^{\boldsymbol{\sigma}}$ contains the multiples of the identity tensor $\mathbb{I}$,

(**H.1**) $\mathbf{div}(\widetilde{\mathbb{H}}_h^{\boldsymbol{\sigma}}) \subseteq \mathbf{H}_h^{\mathbf{u}}$.

As a consequence of (**H.0**) and the decomposition (2.12), $\mathbb{H}_h^{\boldsymbol{\sigma}}$ (cf. (4.1)) can be redefined as

$$\mathbb{H}_h^{\boldsymbol{\sigma}} := \left\{ \boldsymbol{\tau}_h - \left(\frac{1}{n\,|\Omega|} \int_\Omega \mathrm{tr}(\boldsymbol{\tau}_h) \right) \mathbb{I} : \quad \forall\, \boldsymbol{\tau}_h \in \widetilde{\mathbb{H}}_h^{\boldsymbol{\sigma}} \right\} .$$

We remark in advance, however, that for the computational implementation of the Galerkin scheme (4.2) (equivalently (4.3)), which will be addressed later on in Section 6, we will use a real Lagrange multiplier to impose the mean value condition on the trace of the unknown tensor lying in $\mathbb{H}_h^{\boldsymbol{\sigma}}$.

Now, being both a and c symmetric and positive semi-definite on $\mathbb{H}_0(\mathbf{div}_{4/3};\Omega)$ and $\mathbf{L}^4(\Omega)$, respectively, they certainly keep these properties on the corresponding subspaces $\mathbb{H}_h^{\boldsymbol{\sigma}}$ and $\mathbf{H}_h^{\mathbf{u}}$, whence they satisfy the hypothesis **i)** of [15, Theorem 3.5].

In turn, thanks to (**H.1**), $\mathbf{V}_h$ becomes

$$\mathbf{V}_h := \left\{ \boldsymbol{\tau}_h \in \mathbb{H}_h^{\boldsymbol{\sigma}} : \quad \mathbf{div}(\boldsymbol{\tau}_h) = \mathbf{0} \quad \text{in} \quad \Omega \right\}, \tag{4.6}$$

and therefore we conclude the discrete analogue of (3.6) with the same constant from the continuous analysis, that is with $\alpha_{\mathtt{d}} = \alpha := \frac{c_1^2}{\nu}$, which implies

$$\sup_{\mathbf{0} \neq \boldsymbol{\tau}_h \in \mathbf{V}_h} \frac{a(\boldsymbol{\zeta}_h, \boldsymbol{\tau}_h)}{\|\boldsymbol{\tau}_h\|_{\mathbf{div}_{4/3};\Omega}} \geq \alpha_{\mathtt{d}}\, \|\boldsymbol{\zeta}_h\|_{\mathbf{div}_{4/3};\Omega} \quad \forall\, \boldsymbol{\zeta}_h \in \mathbf{V}_h\,, \tag{4.7}$$

thus showing that the hypothesis **ii)** of [15, Theorem 3.5] is also accomplished.

Finally, in order to be able to apply [15, Theorem 3.5], the remaining hypothesis **iii)** of it, that is the discrete inf-sup condition for b, is introduced as an assumption, namely:

(**H.2**) there exists a positive constant $\beta_{\mathtt{d}}$, independent of h, such that

$$\sup_{\mathbf{0} \neq \boldsymbol{\tau}_h \in \mathbb{H}_h^{\boldsymbol{\sigma}}} \frac{b(\boldsymbol{\tau}_h, \mathbf{v}_h)}{\|\boldsymbol{\tau}_h\|_{\mathbf{div}_{4/3};\Omega}} \geq \beta_{\mathtt{d}}\, \|\mathbf{v}_h\|_{0,4;\Omega} \quad \forall\, \mathbf{v}_h \in \mathbf{H}_h^{\mathbf{u}}\,.$$

As already announced, specific finite element subspaces satisfying (**H.0**), (**H.1**), and (**H.2**), will be detailed later on in Section 4.3.

Now, having a, b, and c satisfied the hypotheses of [15, Theorem 3.5], we deduce, similarly to the continuous case (cf. (3.7)), the existence of a constant $\gamma_{\mathtt{d}} > 0$, depending on ν, $\mathtt{D}$, $|\Omega|$, $\alpha_{\mathtt{d}}$, and $\beta_{\mathtt{d}}$, and hence independent of h, such that

$$\sup_{\mathbf{0} \neq (\boldsymbol{\tau}_h, \mathbf{v}_h) \in \mathbf{X}_h} \frac{\mathbf{A}((\boldsymbol{\zeta}_h, \mathbf{z}_h), (\boldsymbol{\tau}_h, \mathbf{v}_h))}{\|(\boldsymbol{\tau}_h, \mathbf{v}_h)\|_{\mathbf{X}}} \geq \gamma_{\mathtt{d}}\, \|(\boldsymbol{\zeta}_h, \mathbf{z}_h)\|_{\mathbf{X}} \quad \forall\, (\boldsymbol{\zeta}_h, \mathbf{z}_h) \in \mathbf{X}_h\,, \tag{4.8}$$

and thus, for each $\mathbf{w}_h \in \mathbf{H}_h^{\mathbf{u}}$ such that $\|\mathbf{w}_h\|_{0,4;\Omega} \leq \widetilde{r}_0$, with

$$\widetilde{r}_0 := \min\{\widetilde{r}_1, \widetilde{r}_2\}\,, \quad \widetilde{r}_1 := \frac{\nu\,\gamma_{\mathtt{d}}}{4}\,, \quad \text{and} \quad \widetilde{r}_2 := \left(\frac{\gamma_{\mathtt{d}}}{4\,\mathtt{F}\,|\Omega|^{(4-\rho)/4}} \right)^{1/(\rho-2)}, \tag{4.9}$$

there holds the discrete version of (3.13), that is

$$\sup_{\mathbf{0} \neq (\boldsymbol{\tau}_h, \mathbf{v}_h) \in \mathbf{X}_h} \frac{\mathbf{A}_{\mathbf{w}_h}((\boldsymbol{\zeta}_h, \mathbf{z}_h), (\boldsymbol{\tau}_h, \mathbf{v}_h))}{\|(\boldsymbol{\tau}_h, \mathbf{v}_h)\|_{\mathbf{X}}} \geq \frac{\gamma_{\mathtt{d}}}{2}\, \|(\boldsymbol{\zeta}_h, \mathbf{z}_h)\|_{\mathbf{X}} \quad \forall\, (\boldsymbol{\zeta}_h, \mathbf{z}_h) \in \mathbf{X}_h\,. \tag{4.10}$$

According to the above and the fact that $\mathbf{F}$ is a linear and bounded functional (cf. (2.20) and (3.4)), a straightforward application of [17, Theorem 2.22] allows to conclude the following result.

Lemma 4.1 *Let $\widetilde{r} \in (0, \widetilde{r}_0]$, with $\widetilde{r}_0$, $\widetilde{r}_1$, and $\widetilde{r}_2$ as in* (4.9)*. Then, for each $\mathbf{w}_h \in \mathbf{H}_h^{\mathbf{u}}$ satisfying $\|\mathbf{w}_h\|_{0,4;\Omega} \leq \widetilde{r}$, the problem* (4.4) *has a unique solution $(\bar{\boldsymbol{\sigma}}_h, \bar{\mathbf{u}}_h) \in \mathbf{X}_h$. Moreover, there holds*

$$\|\mathbf{T}_{\mathtt{d}}(\mathbf{w}_h)\|_{0,4;\Omega} = \|\bar{\mathbf{u}}_h\|_{0,4;\Omega} \leq \|(\bar{\boldsymbol{\sigma}}_h, \bar{\mathbf{u}}_h)\|_{\mathbf{X}} \leq \frac{2\, C_{\mathbf{F}}}{\gamma_{\mathtt{d}}} \left\{ \|\mathbf{f}\|_{0,4/3;\Omega} + \|\mathbf{u}_{\mathrm{D}}\|_{1/2,\Gamma} \right\}, \tag{4.11}$$

with $C_{\mathbf{F}}$ and $\gamma_{\mathtt{d}}$ according to (3.4) *and* (4.8)*, respectively.*

We now proceed to analyze the fixed-point equation (4.5). We begin with the discrete version of Lemma 3.2, whose proof follows straightforwardly from Lemma 4.1.

Lemma 4.2 *Let $\widetilde{r} \in (0, \widetilde{r}_0]$, with $\widetilde{r}_0$, $\widetilde{r}_1$, and $\widetilde{r}_2$ as in* (4.9)*, and let $\mathbf{W}_{\widetilde{r}}$ be the ball of $\mathbf{H}_h^{\mathbf{u}}$ given by*

$$\mathbf{W}_{\widetilde{r}} := \left\{ \mathbf{w}_h \in \mathbf{H}_h^{\mathbf{u}} : \quad \|\mathbf{w}_h\|_{0,4;\Omega} \leq \widetilde{r} \right\}. \tag{4.12}$$

Assume that the data $\mathbf{f}$ and $\mathbf{u}_{\mathrm{D}}$ satisfy

$$\frac{2\, C_{\mathbf{F}}}{\gamma_{\mathtt{d}}} \left\{ \|\mathbf{f}\|_{0,4/3;\Omega} + \|\mathbf{u}_{\mathrm{D}}\|_{1/2,\Gamma} \right\} \leq \widetilde{r}\,, \tag{4.13}$$

with $C_{\mathbf{F}}$ and $\gamma_{\mathtt{d}}$ according to (3.4) *and* (4.8)*, respectively. Then $\mathbf{T}_{\mathtt{d}}(\mathbf{W}_{\widetilde{r}}) \subseteq \mathbf{W}_{\widetilde{r}}$.*

Next, we address the discrete counterpart of Lemma 3.3, whose proof, being almost verbatim to the continuous one, is omitted. Thus, we simply state the corresponding result as follows.

Lemma 4.3 *Let $\rho \in [3, 4]$ and $\widetilde{r} \in (0, \widetilde{r}_0]$, with $\widetilde{r}_0$, $\widetilde{r}_1$, and $\widetilde{r}_2$ as in* (4.9)*, and let $C_{\mathbf{F}}$ and $\gamma_{\mathtt{d}}$ according to* (3.4) *and* (4.8)*, respectively. Then, there holds*

$$\|\mathbf{T}_{\mathtt{d}}(\mathbf{w}_{1,h}) - \mathbf{T}_{\mathtt{d}}(\mathbf{w}_{1,h})\|_{0,4;\Omega} \leq \left(1 + 2^{\rho-3} c_\rho\right) \frac{C_{\mathbf{F}}}{\gamma_{\mathtt{d}}\, \widetilde{r}_0} \left\{ \|\mathbf{f}\|_{0,4/3;\Omega} + \|\mathbf{u}_{\mathrm{D}}\|_{1/2,\Gamma} \right\} \|\mathbf{w}_{1,h} - \mathbf{w}_{2,h}\|_{0,4;\Omega} \tag{4.14}$$

for all $\mathbf{w}_{1,h}$, $\mathbf{w}_{2,h} \in \mathbf{W}_{\widetilde{r}}$.

We are now in position of establishing the well-posedness of (4.3) (equivalently of (4.2)).

Theorem 4.4 *Let $\rho \in [3, 4]$ and $\widetilde{r} \in (0, \widetilde{r}_0]$, with $\widetilde{r}_0$, $\widetilde{r}_1$, and $\widetilde{r}_2$ as in* (4.9)*. Assume that the data satisfy* (4.13) *and*

$$\left(1 + 2^{\rho-3} c_\rho\right) \frac{C_{\mathbf{F}}}{\gamma_{\mathtt{d}}\, \widetilde{r}_0} \left\{ \|\mathbf{f}\|_{0,4/3;\Omega} + \|\mathbf{u}_{\mathrm{D}}\|_{1/2,\Gamma} \right\} < 1\,. \tag{4.15}$$

Then, there exists a unique $\mathbf{u}_h \in \mathbf{W}_{\widetilde{r}}$ (cf. (4.12)*) fixed-point of operator $\mathbf{T}_{\mathtt{d}}$. Equivalently,* (4.3) *(cf.* (4.2)*) has a unique solution $(\boldsymbol{\sigma}_h, \mathbf{u}_h) := (\bar{\boldsymbol{\sigma}}_h, \bar{\mathbf{u}}_h) \in \mathbf{X}_h$ with $\mathbf{u}_h \in \mathbf{W}_{\widetilde{r}}$, where $(\bar{\boldsymbol{\sigma}}_h, \bar{\mathbf{u}}_h)$ is the unique solution of* (4.4) *with $\mathbf{w}_h = \mathbf{u}_h$. Moreover, there holds*

$$\|(\boldsymbol{\sigma}_h, \mathbf{u}_h)\|_{\mathbf{X}} \leq \frac{2\, C_{\mathbf{F}}}{\gamma_{\mathtt{d}}} \left\{ \|\mathbf{f}\|_{0,4/3;\Omega} + \|\mathbf{u}_{\mathrm{D}}\|_{1/2,\Gamma} \right\}. \tag{4.16}$$

Proof. It follows similarly to the proof of Theorem 3.4. Indeed, we first notice from Lemma 4.2 that $\mathbf{T}_{\mathtt{d}}$ maps the ball $\mathbf{W}_{\widetilde{r}}$ into itself. Next, it is easy to see from (4.14) and (4.15) that $\mathbf{T}_{\mathtt{d}}$ is a contraction, and hence the existence and uniqueness results follow from the Banach fixed-point theorem. In addition, it is clear that the estimate (4.16) follows from (4.11), which ends the proof. □

4.3 Specific finite element subspaces

In this section we introduce specific finite element subspaces $\widetilde{\mathbb{H}}_h^{\boldsymbol{\sigma}}$ and $\mathbf{H}_h^{\mathbf{u}}$ satisfying the hypotheses (**H**.**0**), (**H**.**1**) and (**H**.**2**) that were introduced in Section 4.2. These discrete spaces arise naturally as consequence of similar analyses developed in [4] (see also [16] and [19]). Then, with the same notations from Section 4.1, and given an integer $l \geq 0$ and a subset S of $\mathbf{R}$, we denote by $\mathrm{P}_l(S)$ the space of polynomials of total degree at most l defined on S. Hence, for each integer $k \geq 0$ and for each $T \in \mathcal{T}_h$, we define the local Raviart–Thomas space of order k as

$$\mathbf{RT}_k(T) := \mathbf{P}_k(T) \oplus \widetilde{\mathrm{P}}_k(T)\,\mathbf{x}\,,$$

where $\mathbf{x} := (x_1, \ldots, x_n)^{\mathrm{t}}$ is a generic vector of $\mathbf{R}$, $\widetilde{\mathrm{P}}_k(T)$ is the space of polynomials of total degree equal to k defined on T, and, according to the convention in Section 1, we set $\mathbf{P}_k(T) := [\mathrm{P}_k(T)]^n$. Then, denoting by $\boldsymbol{\tau}_{h,i}$ the i-th row of a tensor $\boldsymbol{\tau}_h$, the finite element subspaces on Ω are defined as

$$\begin{aligned} \widetilde{\mathbb{H}}_h^{\boldsymbol{\sigma}} &:= \Big\{ \boldsymbol{\tau}_h \in \mathbb{H}(\mathbf{div}_{4/3};\Omega) : \quad \boldsymbol{\tau}_{h,i}|_T \in \mathbf{RT}_k(T), \quad \forall\, i \in \{1,\ldots,n\}, \quad \forall\, T \in \mathcal{T}_h \Big\}\,, \\ \mathbf{H}_h^{\mathbf{u}} &:= \Big\{ \mathbf{v}_h \in \mathbf{L}^4(\Omega) : \quad \mathbf{v}_h|_T \in \mathbf{P}_k(T)\,, \quad \forall\, T \in \mathcal{T}_h \Big\}\,. \end{aligned} \tag{4.17}$$

It is clear from (4.17) that $\widetilde{\mathbb{H}}_h^{\boldsymbol{\sigma}}$ contains the multiples of the identity tensor $\mathbb{I}$ and that $\mathbf{div}(\widetilde{\mathbb{H}}_h^{\boldsymbol{\sigma}}) \subseteq \mathbf{H}_h^{\mathbf{u}}$, whence (**H**.**0**) and (**H**.**1**) are satisfied. Next, defining $\mathbb{H}_h^{\boldsymbol{\sigma}} := \widetilde{\mathbb{H}}_h^{\boldsymbol{\sigma}} \cap \mathbb{H}_0(\mathbf{div}_{4/3};\Omega)$ as in (4.1), it follows that the bilinear form a (cf. (2.15)) satisfies the inf-sup condition (4.7) on $\mathbf{V}_h$ (cf. (4.6)). In turn, we know from [14, Lemma 5.5] (see also [4, Lemma 4.4] or [6, Lemma 3.3] with $p = 4/3$) that there holds (**H**.**2**).

We end this section by collecting next the approximation properties of the finite element subspaces $\mathbb{H}_h^{\boldsymbol{\sigma}}$ and $\mathbf{H}_h^{\mathbf{u}}$ (cf. (4.17)), whose derivations can be found in [3], [18], and [6, Section 3.1] (see also [14, Section 5.5]):

($\mathbf{AP}_h^{\boldsymbol{\sigma}}$) there exists a positive constant C, independent of h, such that for each $l \in (0, k+1]$ and for each $\boldsymbol{\tau} \in \mathbb{H}^l \cap \mathbb{H}_0(\mathbf{div}_{4/3};\Omega)$ with $\mathbf{div}(\boldsymbol{\tau}) \in \mathbf{W}^{l,4/3}(\Omega)$, there holds

$$\mathrm{dist}\,(\boldsymbol{\tau}, \mathbb{H}_h^{\boldsymbol{\sigma}}) := \inf_{\boldsymbol{\tau}_h \in \mathbb{H}_h^{\boldsymbol{\sigma}}} \|\boldsymbol{\tau} - \boldsymbol{\tau}_h\|_{\mathbf{div}_{4/3};\Omega} \leq C\, h^l \Big\{ \|\boldsymbol{\tau}\|_{l,\Omega} + \|\mathbf{div}(\boldsymbol{\tau})\|_{l,4/3;\Omega} \Big\}\,,$$

($\mathbf{AP}_h^{\mathbf{u}}$) there exists a positive constant C, independent of h, such that for each $l \in [0, k+1]$ and for each $\mathbf{v} \in \mathbf{W}^{l,4}(\Omega)$, there holds

$$\mathrm{dist}\,(\mathbf{v}, \mathbf{H}_h^{\mathbf{u}}) := \inf_{\mathbf{v}_h \in \mathbf{H}_h^{\mathbf{u}}} \|\mathbf{v} - \mathbf{v}_h\|_{0,4;\Omega} \leq C\, h^l\, \|\mathbf{v}\|_{l,4;\Omega}\,.$$

5 A priori error analysis

In this section we first derive the Céa estimate for the Galerkin scheme (4.3) (cf. (4.2)) with the finite element subspaces given by (4.17), and then use the approximation properties of the latter to establish the corresponding rates of convergence. In fact, let $(\boldsymbol{\sigma}, \mathbf{u}) \in \mathbb{H}_0(\mathbf{div}_{4/3};\Omega) \times \mathbf{L}^4(\Omega)$, with $\mathbf{u} \in \mathbf{W}_r$ (cf. (3.14)), be the unique solution of the continuous problem (2.19) (equivalently (2.14)), and let $(\boldsymbol{\sigma}_h, \mathbf{u}_h) \in \mathbb{H}_h^{\boldsymbol{\sigma}} \times \mathbf{H}_h^{\mathbf{u}}$, with $\mathbf{u}_h \in \mathbf{W}_{\widetilde{r}}$ (cf. (4.12)), be the unique solution of the discrete problem (4.3) (equivalently (4.2)). Then, we are interested in deriving an *a priori* estimate for the error

$$\|(\boldsymbol{\sigma}, \mathbf{u}) - (\boldsymbol{\sigma}_h, \mathbf{u}_h)\|_{\mathbf{X}} := \|\boldsymbol{\sigma} - \boldsymbol{\sigma}_h\|_{\mathbf{div}_{4/3};\Omega} + \|\mathbf{u} - \mathbf{u}_h\|_{0,4;\Omega}\,.$$

In what follows, given a subspace X_h of a generic Banach space $(X, \|\cdot\|_X)$, we set for each $x \in X$

$$\mathrm{dist}\,(x, X_h) \,:=\, \inf_{x_h \in X_h} \|x - x_h\|_X .$$

In addition, we let

$$\widehat{r}_0 \,:=\, \min\{\widetilde{r}_1, r_2, \widetilde{r}_2\} \quad \text{and} \quad \widehat{\gamma} \,:=\, \min\{\gamma, \gamma_{\mathtt{d}}\} . \tag{5.1}$$

The main result of this section is established as follows.

Theorem 5.1 *Assume that the data* $\mathbf{f} \in \mathbf{L}^{4/3}(\Omega)$ *and* $\mathbf{u}_{\mathrm{D}} \in \mathbf{H}^{1/2}(\Gamma)$ *satisfy*

$$\big(1 + 2\,c_\rho\big)\,\frac{C_{\mathbf{F}}}{\widehat{\gamma}\,\widehat{r}_0}\,\Big\{\|\mathbf{f}\|_{0,4/3;\Omega} + \|\mathbf{u}_{\mathrm{D}}\|_{1/2,\Gamma}\Big\} \,\leq\, \frac{1}{2} . \tag{5.2}$$

Then, there exists a constant $C > 0$*, independent of* h*, such that*

$$\|(\boldsymbol{\sigma}, \mathbf{u}) - (\boldsymbol{\sigma}_h, \mathbf{u}_h)\|_{\mathbf{X}} \,\leq\, C\,\Big\{\mathrm{dist}\,(\boldsymbol{\sigma}, \mathbb{H}_h^{\boldsymbol{\sigma}}) + \mathrm{dist}\,(\mathbf{u}, \mathbf{H}_h^{\mathbf{u}})\Big\} . \tag{5.3}$$

Proof. Let us first recall from (3.13) and (4.10) that the bounded bilinear forms $\mathbf{A}_{\mathbf{u}}$ and $\mathbf{A}_{\mathbf{u}_h}$ satisfy global inf-sup conditions with constants $\gamma/2$ and $\gamma_{\mathtt{d}}/2$, respectively. In addition, it is clear that $\mathbf{F}$ and $\mathbf{F}|_{\mathbb{H}_h^{\boldsymbol{\sigma}} \times \mathbf{H}_h^{\mathbf{u}}}$ are bounded linear functionals in $\mathbb{H}_0(\mathbf{div}_{4/3}; \Omega) \times \mathbf{L}^4(\Omega)$ and $\mathbb{H}_h^{\boldsymbol{\sigma}} \times \mathbf{H}_h^{\mathbf{u}}$, respectively. It follows that the hypotheses of the Strang-type estimate provided by [9, Lemma 5.1] are satisfied by the continuous and discrete problems given by (2.19) and (4.3), respectively, and hence a straightforward application of this abstract result implies

$$\begin{aligned} \|(\boldsymbol{\sigma}, \mathbf{u}) - (\boldsymbol{\sigma}_h, \mathbf{u}_h)\|_{\mathbf{X}} \,&\leq\, C_1\,\Big\{\mathrm{dist}\,(\boldsymbol{\sigma}, \mathbb{H}_h^{\boldsymbol{\sigma}}) + \mathrm{dist}\,(\mathbf{u}, \mathbf{H}_h^{\mathbf{u}})\Big\} \\ &\quad + C_2\,\big\|\mathbf{B}_{\mathbf{u}}((\boldsymbol{\sigma}, \mathbf{u}), \cdot) - \mathbf{B}_{\mathbf{u}_h}((\boldsymbol{\sigma}, \mathbf{u}), \cdot)\big\|_{(\mathbb{H}_h^{\boldsymbol{\sigma}} \times \mathbf{H}_h^{\mathbf{u}})'} , \end{aligned} \tag{5.4}$$

where, bearing in mind (3.2), C_1 and C_2 are the positive constants given by

$$C_1 \,:=\, 2 + 6\,\frac{C_{\mathbf{A}}}{\gamma_{\mathtt{d}}} + 2\,\frac{\gamma}{\gamma_{\mathtt{d}}} \quad \text{and} \quad C_2 \,:=\, \frac{2}{\gamma_{\mathtt{d}}} . \tag{5.5}$$

Next, proceeding similarly as for the derivation of (3.21), we get

$$\begin{aligned} &\big\|\mathbf{B}_{\mathbf{u}}((\boldsymbol{\sigma}, \mathbf{u}), \cdot) - \mathbf{B}_{\mathbf{u}_h}((\boldsymbol{\sigma}, \mathbf{u}), \cdot)\big\|_{(\mathbb{H}_h^{\boldsymbol{\sigma}} \times \mathbf{H}_h^{\mathbf{u}})'} \\ &\quad \leq\, \left(\frac{1}{\nu} \,+\, \mathtt{F}\,c_\rho\,|\Omega|^{(4-\rho)/4}\,\big(\|\mathbf{u}\|_{0,4;\Omega} + \|\mathbf{u}_h\|_{0,4;\Omega}\big)^{\rho-3}\right)\|\mathbf{u}\|_{0,4;\Omega}\,\|\mathbf{u} - \mathbf{u}_h\|_{0,4;\Omega} . \end{aligned} \tag{5.6}$$

Thus, replacing (5.6) back into (5.4), using the explicit expression of C_2 (cf. (5.5)), the subadditivity inequality for $\rho - 3 \in [0, 1]$, and bounding $\|\mathbf{u}\|_{0,4;\Omega} + \|\mathbf{u}_h\|_{0,4;\Omega}$ by $r_2 + \widetilde{r}_2$, which follows from the fact that $\mathbf{u} \in \mathbf{W}_r$ and $\mathbf{u}_h \in \mathbf{W}_{\widetilde{r}}$, with $r \in (0, r_0]$, $r_0 := \min\{r_1, r_2\}$, $\widetilde{r} \in (0, \widetilde{r}_0]$, and $\widetilde{r}_0 := \min\{\widetilde{r}_1, \widetilde{r}_2\}$ (cf. (3.11), (4.9)), we find that

$$\begin{aligned} &\|(\boldsymbol{\sigma}, \mathbf{u}) - (\boldsymbol{\sigma}_h, \mathbf{u}_h)\|_{\mathbf{X}} \,\leq\, C_1\,\Big\{\mathrm{dist}\,(\boldsymbol{\sigma}, \mathbb{H}_h^{\boldsymbol{\sigma}}) + \mathrm{dist}\,(\mathbf{u}, \mathbf{H}_h^{\mathbf{u}})\Big\} \\ &+ \left(\frac{1}{\gamma\,\widetilde{r}_1} + \left(\frac{1}{\gamma_{\mathtt{d}}\,r_2} + \frac{1}{\gamma\,\widetilde{r}_2}\right)\,c_\rho\right)\,\frac{\gamma}{2}\,\|\mathbf{u}\|_{0,4;\Omega}\,\|\mathbf{u} - \mathbf{u}_h\|_{0,4;\Omega} . \end{aligned}$$

Finally, using the fact that $1/\widetilde{r}_1, 1/r_2, 1/\widetilde{r}_2$ and $1/\gamma, 1/\gamma_{\mathtt{d}}$ are bounded by $1/\widehat{r}_0$ and $1/\widehat{\gamma}$, respectively, with $\widehat{r}_0$ and $\widehat{\gamma}$ defined as in (5.1), bounding $\|\mathbf{u}\|_{0,4;\Omega}$ as in (3.24), and performing simple algebraic manipulations, we get

$$\begin{aligned}\|(\boldsymbol{\sigma},\mathbf{u})-(\boldsymbol{\sigma}_h,\mathbf{u}_h)\|_{\mathbf{X}} \,&\leq\, C_1\left\{\mathrm{dist}\,(\boldsymbol{\sigma},\mathbb{H}_h^{\boldsymbol{\sigma}})+\mathrm{dist}\,(\mathbf{u},\mathbf{H}_h^{\mathbf{u}})\right\}\\ &+\,\big(1+2\,c_\rho\big)\,\frac{C_{\mathbf{F}}}{\widehat{\gamma}\,\widehat{r}_0}\left\{\|\mathbf{f}\|_{0,4/3;\Omega}+\|\mathbf{u}_{\mathrm{D}}\|_{1/2,\Gamma}\right\}\|(\boldsymbol{\sigma},\mathbf{u})-(\boldsymbol{\sigma}_h,\mathbf{u}_h)\|_{\mathbf{X}}\,.\end{aligned}\tag{5.7}$$

Thus, (5.7) in conjunction with the data assumption (5.2), yields (5.3) and ends the proof. □

The following theorem provides the rate of convergences of the Galerkin scheme (4.3) (equivalently (4.2)) under suitable regularity assumptions on the exact solution.

Theorem 5.2 *In addition to the hypotheses of Theorems* 3.4, 4.4, *and* 5.1, *assume that there exists* $l\in(0,k+1]$ *such that* $\boldsymbol{\sigma}\in\mathbb{H}^l(\Omega)\cap\mathbb{H}_0(\mathbf{div}_{4/3};\Omega)$, $\mathbf{div}(\boldsymbol{\sigma})\in\mathbf{W}^{l,4/3}(\Omega)$, *and* $\mathbf{u}\in\mathbf{W}^{l,4}(\Omega)$. *Then, there exists a constant* $C>0$, *independent of* h, *such that*

$$\|(\boldsymbol{\sigma},\mathbf{u})-(\boldsymbol{\sigma}_h,\mathbf{u}_h)\|\,\leq\,C\,h^l\left\{\|\boldsymbol{\sigma}\|_{l,\Omega}+\|\mathbf{div}(\boldsymbol{\sigma})\|_{l,4/3;\Omega}+\|\mathbf{u}\|_{l,4;\Omega}\right\}.$$

Proof. It follows from a direct application of Theorem 5.1 and the approximation properties $(\mathbf{AP}_h^{\boldsymbol{\sigma}})$ and $(\mathbf{AP}_h^{\mathbf{u}})$ specified in Section 4.3. □

We end this section by introducing suitable approximations for the pressure p, the velocity gradient $\mathbf{G}:=\nabla\mathbf{u}$, the vorticity $\boldsymbol{\omega}:=\frac{1}{2}\big(\nabla\mathbf{u}-(\nabla\mathbf{u})^{\mathrm{t}}\big)$, and the shear stress tensor $\widetilde{\boldsymbol{\sigma}}:=\nu\big(\nabla\mathbf{u}+(\nabla\mathbf{u})^{\mathrm{t}}\big)-p\,\mathbb{I}$, all them of physical interest. Indeed, the continuous expressions provided in (2.4) and (2.6), and the decomposition of the original unknown $\boldsymbol{\sigma}$ given by (2.13), suggest the following discrete formulae in terms of the solution $(\boldsymbol{\sigma}_h,\mathbf{u}_h)\in\mathbb{H}_h^{\boldsymbol{\sigma}}\times\mathbf{H}_h^{\mathbf{u}}$ of problem (4.2):

$$\begin{aligned}&p_h=-\frac{1}{n}\mathrm{tr}(\boldsymbol{\sigma}_h+\mathbf{u}_h\otimes\mathbf{u}_h)-c_{0,h},\quad \mathbf{G}_h=\frac{1}{\nu}\big(\boldsymbol{\sigma}_h^{\mathrm{d}}+(\mathbf{u}_h\otimes\mathbf{u}_h)^{\mathrm{d}}\big),\quad \boldsymbol{\omega}_h=\frac{1}{2\nu}\big(\boldsymbol{\sigma}_h-\boldsymbol{\sigma}_h^{\mathrm{t}}\big),\ \text{and}\\ &\widetilde{\boldsymbol{\sigma}}_h=\boldsymbol{\sigma}_h^{\mathrm{d}}+(\mathbf{u}_h\otimes\mathbf{u}_h)^{\mathrm{d}}+\boldsymbol{\sigma}_h^{\mathrm{t}}+(\mathbf{u}_h\otimes\mathbf{u}_h)+c_{0,h}\,\mathbb{I},\quad\text{with}\quad c_{0,h}=-\frac{1}{n\,|\Omega|}\int_\Omega\mathrm{tr}(\mathbf{u}_h\otimes\mathbf{u}_h)\,.\end{aligned}\tag{5.8}$$

The following result establishes the rates of convergence for these additional variables.

Lemma 5.3 *Assume that there exists* $l\in(0,k+1]$ *such that* $\boldsymbol{\sigma}\in\mathbb{H}^l(\Omega)\cap\mathbb{H}_0(\mathbf{div}_{4/3};\Omega)$, $\mathbf{div}(\boldsymbol{\sigma})\in\mathbf{W}^{l,4/3}(\Omega)$, *and* $\mathbf{u}\in\mathbf{W}^{l,4}(\Omega)$. *Then, there exists a constant* $C>0$, *independent of* h, *such that*

$$\begin{aligned}&\|p-p_h\|_{0,\Omega}+\|\mathbf{G}-\mathbf{G}_h\|_{0,\Omega}+\|\boldsymbol{\omega}-\boldsymbol{\omega}_h\|_{0,\Omega}+\|\widetilde{\boldsymbol{\sigma}}-\widetilde{\boldsymbol{\sigma}}_h\|_{0,\Omega}\\ &\qquad\leq\,C\,h^l\left\{\|\boldsymbol{\sigma}\|_{l,\Omega}+\|\mathbf{div}(\boldsymbol{\sigma})\|_{l,4/3;\Omega}+\|\mathbf{u}\|_{l,4;\Omega}\right\}.\end{aligned}$$

Proof. Adding and subtracting $\mathbf{u}\otimes\mathbf{u}_h$ (also works with $\mathbf{u}_h\otimes\mathbf{u}$) to estimate $\|(\mathbf{u}\otimes\mathbf{u})-(\mathbf{u}_h\otimes\mathbf{u}_h)\|_{0,\Omega}$ whenever needed, and employing the triangle and Hölder inequalities, one easily derives the existence of a constant $C>0$, depending only on data and other constants, all of them independent of h, such that

$$\begin{aligned}&\|p-p_h\|_{0,\Omega}+\|\mathbf{G}-\mathbf{G}_h\|_{0,\Omega}+\|\boldsymbol{\omega}-\boldsymbol{\omega}_h\|_{0,\Omega}+\|\widetilde{\boldsymbol{\sigma}}-\widetilde{\boldsymbol{\sigma}}_h\|_{0,\Omega}\\ &\qquad\leq\,C\left\{\|\boldsymbol{\sigma}-\boldsymbol{\sigma}_h\|_{\mathbf{div}_{4/3};\Omega}+\big(\|\mathbf{u}\|_{0,4;\Omega}+\|\mathbf{u}_h\|_{0,4;\Omega}\big)\|\mathbf{u}-\mathbf{u}_h\|_{0,4;\Omega}\right\}.\end{aligned}\tag{5.9}$$

Then, using that $\mathbf{u}\in\mathbf{W}_r$ and $\mathbf{u}_h\in\mathbf{W}_{\widetilde{r}}$, the result follows from (5.9) and Theorem 5.2. □

6 Numerical results

In this section we present three examples illustrating the performance of the mixed finite element method (4.2) on a set of quasi-uniform triangulations of the respective domains, and considering the finite element subspaces defined by (4.17) (cf. Section 4.3). In what follows, we refer to the corresponding sets of finite element subspaces generated by $k = 0$ and $k = 1$, as simply $\mathbb{RT}_0 - \mathbf{P}_0$ and $\mathbb{RT}_1 - \mathbf{P}_1$, respectively. The implementation of the numerical method is based on a `FreeFem++` code [22]. A Newton–Raphson algorithm with a fixed tolerance $\mathsf{tol} = 1\mathrm{E}-6$ is used for the resolution of the nonlinear problem (4.2). As usual, the iterative method is finished when the relative error between two consecutive iterations of the complete coefficient vector, namely $\mathbf{coeff}^m$ and $\mathbf{coeff}^{m+1}$, is sufficiently small, that is,

$$\frac{\|\mathbf{coeff}^{m+1} - \mathbf{coeff}^m\|_{\mathtt{DOF}}}{\|\mathbf{coeff}^{m+1}\|_{\mathtt{DOF}}} \leq \mathsf{tol}\,,$$

where $\|\cdot\|_{\mathtt{DOF}}$ stands for the usual Euclidean norm in $\mathrm{R}^{\mathtt{DOF}}$ with `DOF` denoting the total number of degrees of freedom defining the finite element subspaces $\mathbb{H}_h^{\boldsymbol{\sigma}}$ and $\mathbf{H}_h^{\mathbf{u}}$ (cf. (4.17)).

We now introduce some additional notation. The individual errors are denoted by

$$\mathsf{e}(\boldsymbol{\sigma}) := \|\boldsymbol{\sigma} - \boldsymbol{\sigma}_h\|_{\mathbf{div}_{4/3};\Omega}, \quad \mathsf{e}(\mathbf{u}) := \|\mathbf{u} - \mathbf{u}_h\|_{0,4;\Omega}, \quad \mathsf{e}(p) := \|p - p_h\|_{0,\Omega},$$

$$\mathsf{e}(\mathbf{G}) := \|\mathbf{G} - \mathbf{G}_h\|_{0,\Omega}, \quad \mathsf{e}(\boldsymbol{\omega}) := \|\boldsymbol{\omega} - \boldsymbol{\omega}_h\|_{0,\Omega}, \quad \mathsf{e}(\widetilde{\boldsymbol{\sigma}}) := \|\widetilde{\boldsymbol{\sigma}} - \widetilde{\boldsymbol{\sigma}}_h\|_{0,\Omega}\,,$$

and, as usual, for each $\star \in \{\boldsymbol{\sigma}, \mathbf{u}, p, \mathbf{G}, \boldsymbol{\omega}, \widetilde{\boldsymbol{\sigma}}\}$ we let $\mathsf{r}(\star)$ be the experimental rate of convergence given by $\mathsf{r}(\star) := \log\big(\mathsf{e}(\star)/\widehat{\mathsf{e}}(\star)\big)/\log(h/\widehat{h})$, where h and $\widehat{h}$ denote two consecutive meshsizes with errors e and $\widehat{\mathsf{e}}$, respectively.

The examples to be considered in this section are described next. In all of them, for sake of simplicity, we take $\nu = 1$. In addition, as was already announced in Section 4.2, the null mean value of $\mathrm{tr}(\boldsymbol{\sigma}_h)$ over Ω is fixed via a real Lagrange multiplier strategy.

Example 1: 2D smooth exact solution with varying `D` and `F` parameters

In this test we corroborate the rates of convergence in a two-dimensional domain and also study the performance of the numerical method with respect to the number of Newton iterations required to achieve certain tolerance when different values of the parameters `D` and `F` are given. The domain is the square $\Omega = (0,1)^2$. We choose the inertial power $\rho = 3$, and adjust the datum $\mathbf{f}$ in (2.5) such that the exact solution is given by

$$\mathbf{u}(x_1, x_2) = \begin{pmatrix} \sin(\pi x_1)\cos(\pi x_2) \\ -\cos(\pi x_1)\sin(\pi x_2) \end{pmatrix}, \quad p(x_1, x_2) = \cos(\pi x_1)\sin\left(\frac{\pi}{2}x_2\right).$$

The model problem is then complemented with the appropriate Dirichlet boundary condition. Tables 6.1 and 6.2 show the convergence history for a sequence of quasi-uniform mesh refinements, including the number of Newton iterations when `D` $= 1$ and `F` $= 10$. Notice that we are able not only to approximate the original unknowns but also the pressure field, the velocity gradient, the vorticity and the shear stress tensor through the formulae (5.8). The results confirm that the optimal rates of convergence $\mathcal{O}(h^{k+1})$ predicted by Theorem 5.2 and Lemma 5.3 are attained for $k = 0, 1$. The Newton method exhibits a behavior independent of the meshsize, converging in four iterations in all cases. In Figure 6.1 we display some solutions obtained with the mixed $\mathbb{RT}_1 - \mathbf{P}_1$ approximation with meshsize $h = 0.0128$ and $39,146$ triangle elements (actually representing $627,360$ `DOF`). On the other

hand, in Table 6.3 we report the number of Newton iterations as a function of the parameters D and F, considering polynomial degree $k = 0$ and different meshsizes h. We can observe that Newton's method is robust with respect to both h and D, while the number of iterations increases for larger values of F due to the increasing weight of the nonlinear term $\mathtt{F}\,|\mathbf{u}|\mathbf{u}$.

Example 2: Convergence against smooth exact solutions in a 3D domain

In the second example we consider the cube domain $\Omega = (0,1)^3$ and the parameters $\mathtt{D} = 1, \mathtt{F} = 10$ and $\rho = 3.5$. The manufactured solution is given by

$$\mathbf{u}(x_1,x_2,x_3) = \begin{pmatrix} \sin(\pi x_1)\cos(\pi x_2)\cos(\pi x_3) \\ -2\cos(\pi x_1)\sin(\pi x_2)\cos(\pi x_3) \\ \cos(\pi x_1)\cos(\pi x_2)\sin(\pi x_3) \end{pmatrix}, \quad p(x_1,x_2,x_3) = \cos(\pi x_1)\exp(x_2+x_3)\,.$$

Similarly to the first example, the data $\mathbf{f}$ and $\mathbf{u}_{\mathrm{D}}$ are computed from (2.5) using the above solution. The convergence history for a set of quasi-uniform mesh refinements using $k = 0$ is shown in Table 6.4. Again, the mixed finite element method converges optimally with order $\mathcal{O}(h)$, as it was proved by Theorem 5.2 and Lemma 5.3. In addition, some components of the numerical solution are displayed in Figure 6.2, which were built using the mixed $\mathbb{RT}_0 - \mathbf{P}_0$ approximation with meshsize $h = 0.0786$ and $34,992$ tetrahedral elements (actually representing $320,760\,\mathtt{DOF}$).

Example 3: Flow through a 2D porous media with fracture network.

Inspired by [11, Example 4, Section 6], we finally focus on a flow through a porous medium with a fracture network considering strong jump discontinuities of the parameters D and F across the two regions. We consider the square domain $\Omega = (-1,1)^2$ with an internal fracture network denoted as Ω_{f} (see Figure 6.3 below), and boundary Γ, whose left, right, upper and lower parts are given by $\Gamma_{\mathrm{left}} = \{-1\} \times (-1,1)$, $\Gamma_{\mathrm{right}} = \{1\} \times (-1,1)$, $\Gamma_{\mathrm{top}} = (-1,1) \times \{1\}$, and $\Gamma_{\mathrm{bottom}} = (-1,1) \times \{-1\}$, respectively. Note that the boundary of the internal fracture network is defined as a union of segments. The prescribed mesh file is available in `https://github.com/scaucao/Fracture_network-prescribed-mesh`. We consider the convective Brinkman–Forchheimer equations (2.5) in the whole domain Ω, with inertial power $\rho = 4$ but with different values of the parameters D and F for the interior and the exterior of the fracture, namely

$$\mathtt{F} = \begin{cases} 10 & \text{in} \quad \Omega_{\mathrm{f}} \\ 1 & \text{in} \quad \overline{\Omega} \setminus \Omega_{\mathrm{f}} \end{cases} \quad \text{and} \quad \mathtt{D} = \begin{cases} 1 & \text{in} \quad \Omega_{\mathrm{f}} \\ 1000 & \text{in} \quad \overline{\Omega} \setminus \Omega_{\mathrm{f}} \end{cases} . \tag{6.1}$$

The parameter choice corresponds to increased inertial effect ($\mathtt{F} = 10$) in the fracture and a high permeability ($\mathtt{D} = 1$), compared to reduced inertial effect ($\mathtt{F} = 1$) in the porous medium and low permeability ($\mathtt{D} = 1000$). In turn, the body force term is $\mathbf{f} = \mathbf{0}$ and the boundaries conditions are detailed in (6.2), which drives the flow in a diagonal direction from the left-bottom corner to the right-top corner of the square domain Ω.

In Figure 6.4, we display the prescribed quasi-uniform mesh, the computed magnitude of the velocity, velocity gradient tensor, and pseudostress tensor, which were built using the $\mathbb{RT}_1 - \mathbf{P}_1$ scheme on a mesh with $h = 0.0288$ and $31,932$ triangle elements (actually representing $511,872\,\mathtt{DOF}$). We note that the velocity in the fractures is higher than the velocity in the porous medium, due to smaller fractures thickness and the parameter setting (6.1). Also, the velocity is higher in branches of the network where the fluid enters from the left-bottom corner and decreases toward the right-top corner of the

DOF	h	e($\boldsymbol{\sigma}$)	r($\boldsymbol{\sigma}$)	e($\mathbf{u}$)	r($\mathbf{u}$)	e(p)	r(p)
196	0.3727	4.43E-00	–	2.49E-01	–	3.65E-01	–
792	0.1964	1.94E-00	1.285	1.09E-01	1.292	1.54E-01	1.345
3084	0.0970	9.72E-01	0.983	5.45E-02	0.980	7.28E-02	1.065
12208	0.0478	4.74E-01	1.013	2.63E-02	1.029	3.42E-02	1.068
48626	0.0245	2.40E-01	1.023	1.34E-02	1.011	1.77E-02	0.984
196242	0.0128	1.18E-01	1.077	6.63E-03	1.077	8.54E-03	1.117

e($\mathbf{G}$)	r($\mathbf{G}$)	e($\boldsymbol{\omega}$)	r($\boldsymbol{\omega}$)	e($\widetilde{\boldsymbol{\sigma}}$)	r($\widetilde{\boldsymbol{\sigma}}$)	iter
7.24E-01	–	3.99E-01	–	1.32E-00	–	4
3.40E-01	1.183	1.91E-01	1.152	6.03E-01	1.218	4
1.73E-01	0.958	1.00E-01	0.912	3.00E-01	0.991	4
8.65E-02	0.977	5.14E-02	0.944	1.47E-01	1.002	4
4.32E-02	1.038	2.52E-02	1.067	7.46E-02	1.019	4
2.14E-02	1.075	1.27E-02	1.054	3.67E-02	1.089	4

Table 6.1: [Example 1] Number of degrees of freedom, meshsizes, errors, rates of convergence, and number of Newton iterations for the mixed $\mathbb{RT}_0 - \mathbf{P}_0$ approximation of the convective Brinkman–Forchheimer model with $\mathtt{D} = 1$, $\mathtt{F} = 10$, and $\rho = 3$.

domain. In addition, we observe a sharp velocity gradient across the interfaces between the fractures and the porous medium. The pseudostress is consistent with the boundary conditions (6.2) and it is more diffused since it includes the pressure field. This example illustrates the ability of the method to provide accurate resolution and numerically stable results for heterogeneous inclusions with high aspect ratio and complex geometry, as presented in the network of thin fractures. We notice that the mesh used in this example was built by considering a quasi-uniform refinement. Nevertheless, this refinement can be improved and automatized by employing a suitable *a posteriori* error indicator as in [8] that captures the aforementioned discontinuity of the parameters and localize the refinement where it is needed. The corresponding *a posteriori* error analysis and numerical implementation will be addressed in a future work.

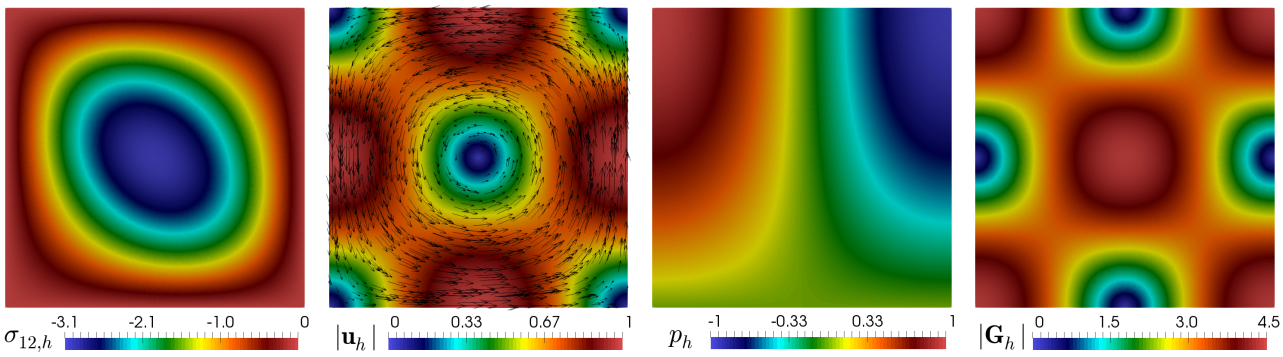

Figure 6.1: [Example 1] Computed pseudostress tensor component, magnitude of the velocity, pressure field and magnitude of the velocity gradient tensor.

DOF	h	e($\boldsymbol{\sigma}$)	r($\boldsymbol{\sigma}$)	e($\mathbf{u}$)	r($\mathbf{u}$)	e(p)	r(p)
608	0.3727	5.31E-01	–	2.66E-02	–	5.35E-02	–
2496	0.1964	1.23E-01	2.286	6.68E-03	2.159	9.78E-03	2.652
9792	0.0970	3.12E-02	1.941	1.67E-03	1.963	2.42E-03	1.982
38912	0.0478	7.90E-03	1.942	4.32E-04	1.913	5.72E-04	2.035
155296	0.0245	1.99E-03	2.066	1.08E-04	2.070	1.47E-04	2.037
627360	0.0128	4.83E-04	2.167	2.63E-05	2.169	3.54E-05	2.178

e($\mathbf{G}$)	r($\mathbf{G}$)	e($\boldsymbol{\omega}$)	r($\boldsymbol{\omega}$)	e($\widetilde{\boldsymbol{\sigma}}$)	r($\widetilde{\boldsymbol{\sigma}}$)	iter
9.74E-02	–	5.48E-02	–	1.78E-01	–	4
1.80E-02	2.640	9.27E-03	2.775	3.37E-02	2.596	4
4.60E-03	1.933	2.33E-03	1.960	8.63E-03	1.933	4
1.09E-03	2.036	5.41E-04	2.061	2.05E-03	2.029	4
2.80E-04	2.033	1.39E-04	2.037	5.28E-04	2.032	4
6.87E-05	2.153	3.45E-05	2.134	1.29E-04	2.162	4

Table 6.2: [Example 1] Number of degrees of freedom, meshsizes, errors, rates of convergence, and number of Newton iterations for the mixed $\mathbb{RT}_1 - \mathbf{P}_1$ approximation of the convective Brinkman–Forchheimer model with $\mathtt{D} = 1$, $\mathtt{F} = 10$, and $\rho = 3$.

D	F	$h = 0.3727$	$h = 0.1964$	$h = 0.0970$	$h = 0.0478$	$h = 0.0245$	$h = 0.0128$
1	1	4	4	4	4	4	4
10^1	1	4	4	4	4	4	4
10^2	1	4	4	3	3	3	3
10^3	1	3	3	3	3	3	3
1	10^1	4	4	4	4	4	4
1	10^2	6	6	6	6	6	6
1	10^3	9	9	9	9	9	9

Table 6.3: [Example 1] Performance of the iterative method (number of Newton iterations) upon variations of the parameters D and F with polynomial degree $k = 0$ and $\rho = 3$.

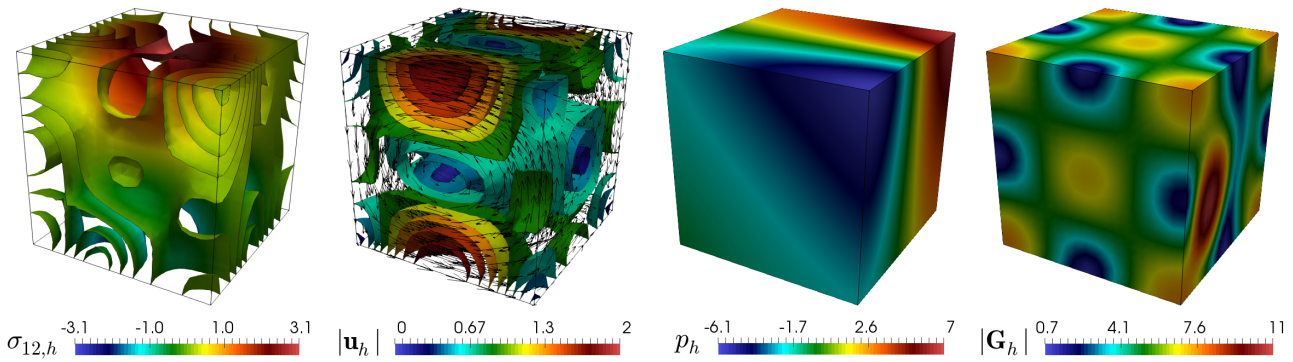

Figure 6.2: [Example 2] Computed pseudostress tensor component, magnitude of the velocity, pressure field and magnitude of the velocity gradient tensor.

DOF	h	e($\boldsymbol{\sigma}$)	r($\boldsymbol{\sigma}$)	e($\mathbf{u}$)	r($\mathbf{u}$)	e(p)	r(p)
504	0.7071	1.54E+01	–	5.66E-01	–	1.26E-00	–
1620	0.4714	1.07E+01	0.900	3.93E-01	0.898	9.13E-01	0.784
12312	0.2357	5.47E-00	0.968	2.06E-01	0.936	4.54E-01	1.009
74052	0.1286	2.97E-00	1.006	1.13E-01	0.984	2.22E-01	1.180
320760	0.0786	1.81E-00	1.012	6.93E-02	0.995	1.23E-01	1.206

e($\mathbf{G}$)	r($\mathbf{G}$)	e($\boldsymbol{\omega}$)	r($\boldsymbol{\omega}$)	e($\widetilde{\boldsymbol{\sigma}}$)	r($\widetilde{\boldsymbol{\sigma}}$)	iter
2.31E-00	–	1.52E-00	–	4.10E-00	–	4
1.60E-00	0.906	1.04E-00	0.935	2.90E-00	0.856	4
8.36E-01	0.937	5.32E-01	0.970	1.51E-00	0.941	4
4.65E-01	0.968	2.92E-01	0.988	8.19E-01	1.009	4
2.86E-01	0.984	1.79E-01	0.995	4.95E-01	1.023	4

Table 6.4: [Example 2] Number of degrees of freedom, meshsizes, errors, rates of convergence, and number of Newton iterations for the mixed $\mathbb{RT}_0 - \mathbf{P}_0$ approximation of the convective Brinkman–Forchheimer model with $\mathtt{D} = 1, \mathtt{F} = 10$, and $\rho = 3.5$.

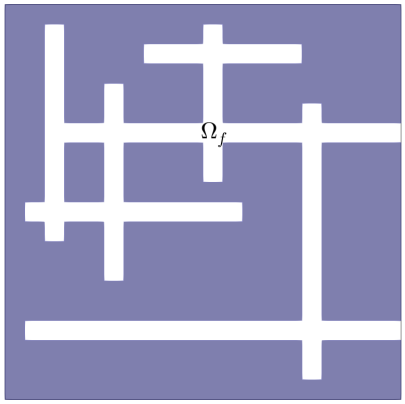

$$\boldsymbol{\sigma}\,\mathbf{n} = \begin{cases} (-0.5(x_2-1),\,0)^{\mathrm{t}} & \text{on} \quad \Gamma_{\mathrm{left}}\,, \\ (0,\,-0.5(x_1-1))^{\mathrm{t}} & \text{on} \quad \Gamma_{\mathrm{bottom}}\,, \end{cases} \qquad (6.2)$$

$$\boldsymbol{\sigma}\,\mathbf{n} = (0,\,0)^{\mathrm{t}} \quad \text{on} \quad \Gamma_{\mathrm{right}} \cup \Gamma_{\mathrm{top}}\,,$$

Figure 6.3: [Example 3] Left: computational domain. Right: boundary conditions.

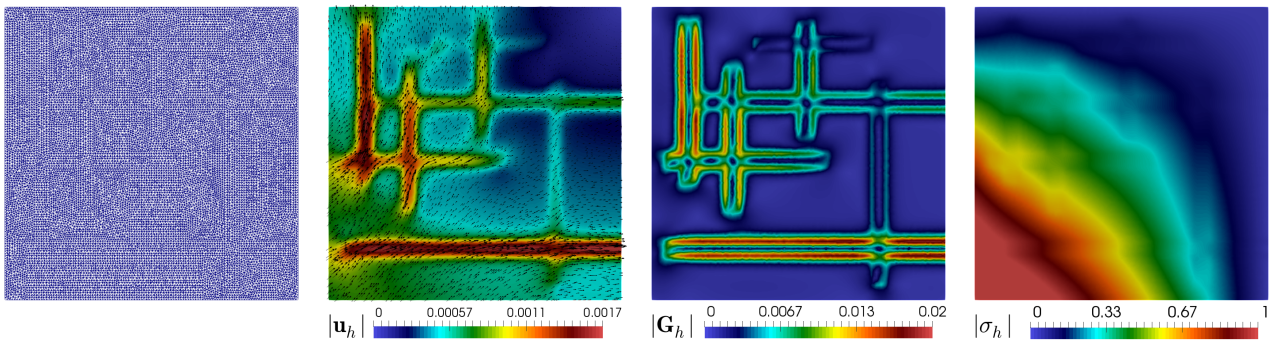

Figure 6.4: [Example 3] Prescribed quasi-uniform mesh, computed magnitude of the velocity, velocity gradient tensor, and pseudostress tensor.

References

[1] G.A. Benavides, S. Caucao, G.N. Gatica and A.A. Hopper, *A Banach spaces-based analysis of a new mixed-primal finite element method for a coupled flow-transport problem*. Comput. Methods Appl. Mech. Engrg. 371 (2020), 113285, 29 pp.

[2] G.A. Benavides, S. Caucao, G.N. Gatica and A.A. Hopper, *A new non-augmented and momentum-conserving fully-mixed finite element method for a coupled flow-transport problem*. Calcolo 59 (2022), no. 1, Paper No. 6, 44 pp.

[3] F. Brezzi and M. Fortin, *Mixed and Hybrid Finite Element Methods*. Springer Series in Computational Mathematics, 15. Springer-Verlag, New York, 1991.

[4] J. Camaño, C. García and R. Oyarzúa, *Analysis of a momentum conservative mixed-FEM for the stationary Navier-Stokes problem*. Numer. Methods Partial Differential Equations 37 (2021), no. 5, 2895–2923.

[5] J. Camaño, G.N. Gatica, R. Oyarzúa and G. Tierra, *An augmented mixed finite element method for the Navier-Stokes equations with variable viscosity*. SIAM J. Numer. Anal. 54 (2016), no. 2, 1069–1092.

[6] J. Camaño, C. Muñoz and R. Oyarzúa, *Numerical analysis of a dual-mixed problem in non-standard Banach spaces*. Electron. Trans. Numer. Anal. 48 (2018), 114–130.

[7] S. Caucao, E. Colmenares, G.N. Gatica and C. Inzunza, *A Banach spaces-based fully-mixed finite element method for the stationary chemotaxis-Navier-Stokes problem*. Preprint 2022-16, Centro de Investigación en Ingeniería Matemática, Universidad de Concepción, Concepción, Chile, (2022).

[8] S. Caucao and J. Esparza, *An augmented mixed FEM for the convective Brinkman–Forchheimer problem: a priori and a posteriori error analysis*. arXiv:2209.02894 [math.NA], (2023).

[9] S. Caucao, G.N. Gatica, R. Oyarzúa and N. Sánchez, *A fully-mixed formulation for the steady double-diffusive convection system based upon Brinkman–Forchheimer equations*. J. Sci. Comput. 85 (2020), no. 2, Paper No. 44, 37 pp.

[10] S. Caucao, R. Oyarzúa and S. Villa-Fuentes, *A new mixed-FEM for steady-state natural convection models allowing conservation of momentum and thermal energy*. Calcolo 57 (2020), no. 4, Paper No. 36, 39 pp.

[11] S. Caucao, R. Oyarzúa, S. Villa-Fuentes and I. Yotov, *A three-field Banach spaces-based mixed formulation for the unsteady Brinkman–Forchheimer equations*. Comput. Methods Appl. Mech. Engrg. 394 (2022), Paper No. 114895, 32 pp.

[12] S. Caucao and I. Yotov, *A Banach space mixed formulation for the unsteady Brinkman-Forchheimer equations*. IMA J. Numer. Anal. 41 (2021), no. 4, 2708–2743.

[13] A.O. Celebi, V.K. Kalantarov and D. Ugurlu, *Continuous dependence for the convective Brinkman–Forchheimer equations*. Appl. Anal. 84 (2005), no. 9, 877–888.

[14] E. Colmenares, G.N. Gatica and S. Moraga, *A Banach spaces-based analysis of a new fully-mixed finite element method for the Boussinesq problem*. ESAIM Math. Model. Numer. Anal. 54 (2020), no. 5, 1525–1568.

[15] C.I. Correa and G.N. Gatica, *On the continuous and discrete well-posedness of perturbed saddle-point formulations in Banach spaces*. Comput. Math. Appl. 117 (2022), 14–23.

[16] C.I. Correa, G.N. Gatica and R. Ruiz-Baier, *New mixed finite element methods for the coupled Stokes and Poisson-Nernst-Planck equations in Banach spaces*. ESAIM Math. Model. Numer. Anal., https://doi.org/10.1051/m2an/2023024.

[17] A. Ern and J.-L. Guermond, *Theory and Practice of Finite Elements*. Applied Mathematical Sciences, 159. Springer-Verlag, New York, 2004.

[18] G.N. Gatica, *A Simple Introduction to the Mixed Finite Element Method. Theory and Applications*. SpringerBriefs in Mathematics. Springer, Cham, 2014.

[19] G.N. Gatica, N. Núñez and R. Ruiz-Baier, *New non-augmented mixed finite element methods for the Navier–Stokes–Brinkman equations using Banach spaces*. J. Numer. Math., https://doi.org/10.1515/jnma-2022-0073.

[20] L.F. Gatica, R. Oyarzúa and N. Sánchez, *A priori and a posteriori error analysis of an augmented mixed-FEM for the Navier-Stokes-Brinkman problem*. Comput. Math. Appl. 75 (2018), no. 7, 2420–2444.

[21] R. Glowinski and A. Marrocco, *Sur l'approximation, par éléments finis d'ordre un, et la résolution, par pénalisations-dualité d'une classe de problémes de Dirichlet non lineaires*. R.A.I.R.O. tome 9, no 2 (1975), p. 41-76.

[22] F. Hecht, *New development in FreeFem++*. J. Numer. Math. 20 (2012), 251-–265.

[23] D. Liu and K. Li, *Mixed finite element for two-dimensional incompressible convective Brinkman-Forchheimer equations*. Appl. Math. Mech. (English Ed.) 40 (2019), no. 6, 889–910.

[24] H. Yu, *Axisymmetric solutions to the convective Brinkman-Forchheimer equations*. J. Math. Anal. Appl. 520 (2023), no. 2, Paper No. 126892, 12 pp.

[25] C. Zhao and Y. You, *Approximation of the incompressible convective Brinkman–Forchheimer equations*. J. Evol. Equ. 12 (2012), no. 4, 767–788.

Centro de Investigación en Ingeniería Matemática (CI^{2}MA)

PRE-PUBLICACIONES 2022 - 2023

2022-36 Gabriel R. Barrenechea, Antonio Tadeu A. Gomes, Diego Paredes: *A Multiscale Hybrid Method*

2022-37 Rodrigo Abarca Del Rio, Fernando Campos, Dieter Issler, Mauricio Sepúlveda: *Study of Avalanche Models Using Well Balanced Finite Volume Schemes*

2023-01 Julio Careaga, Gabriel N. Gatica: *Coupled mixed finite element and finite volume methods for a solid velocity-based model of multidimensional settling*

2023-02 Theophile Chaumont Frelet, Diego Paredes, Frederic Valentin: *Flux approximation on unfitted meshes and application to multiscale hybrid-mixed methods*

2023-03 Esteban Henriquez, Manuel Solano: *An unfitted HDG method for a distributed optimal control problem*

2023-04 Laurence Beaude, Franz Chouly, Mohamed Laaziri, Roland Masson: *Mixed and Nitsche's discretizations of Coulomb frictional contact-mechanics for mixed dimensional poromechanical models*

2023-05 Paola Goatin, Luis M. Villada, Alexandra Würth: *A cheap and easy-to-implement upwind scheme for second order traffic flow models*

2023-06 Franz Chouly, Guillaume Drouet, Hao Huang, Nicolás Pignet: *HHT-α and TR-BDF2 schemes for dynamic contact problems*

2023-07 Paola Goatin, Daniel Inzunza, Luis M. Villada: *Numerical comparison of nonlocal macroscopic models of multi-population pedestrian flows with anisotropic kernel*

2023-08 Lady Angelo, Jessika Camaño, Sergio Caucao: *A five-field mixed formulation for stationary magnetohydrodynamic flows in porous media*

2023-09 Rodolfo Araya, Franz Chouly: *Residual a posteriori error estimation for frictional contact with Nitsche method*

2023-10 Sergio Caucao, Gabriel N. Gatica, Luis F. Gatica: *A Banach spaces-based mixed finite element method for the stationary convective Brinkman-Forchheimer problem*

Para obtener copias de las Pre-Publicaciones, escribir o llamar a: Director, Centro de Investigación en Ingeniería Matemática, Universidad de Concepción, Casilla 160-C, Concepción, Chile, Tel.: 41-2661324, o bien, visitar la página web del centro: http://www.ci2ma.udec.cl







Centro de Investigación en
Ingeniería Matemática (CI²MA)
Universidad de Concepción

Casilla 160-C, Concepción, Chile
Tel.: 56-41-2661324/2661554/2661316
http://www.ci2ma.udec.cl